



**HAL**  
open science

## Oxytocin receptor agonist reduces perinatal brain damage by targeting microglia

Jérôme Mairesse, Manuela Zinni, Julien Pansiot, Rahma Hassan-Abdi, Charlie Demené, Marina Colella, Christiane Charriaut-Marlangue, Aline Rideau Batista Novais, Mickael Tanter, Stefania Maccari, et al.

### ► To cite this version:

Jérôme Mairesse, Manuela Zinni, Julien Pansiot, Rahma Hassan-Abdi, Charlie Demené, et al.. Oxytocin receptor agonist reduces perinatal brain damage by targeting microglia. *Glia*, 2019, 67 (2), pp.345-359. 10.1002/glia.23546 . inserm-04075780

**HAL Id: inserm-04075780**

**<https://inserm.hal.science/inserm-04075780>**

Submitted on 20 Apr 2023

**HAL** is a multi-disciplinary open access archive for the deposit and dissemination of scientific research documents, whether they are published or not. The documents may come from teaching and research institutions in France or abroad, or from public or private research centers.

L'archive ouverte pluridisciplinaire **HAL**, est destinée au dépôt et à la diffusion de documents scientifiques de niveau recherche, publiés ou non, émanant des établissements d'enseignement et de recherche français ou étrangers, des laboratoires publics ou privés.

## **Oxytocin receptor agonist reduces perinatal brain damage by targeting neuroinflammation**

Jérôme Mairesse<sup>1, 2</sup>, Manuela Zinni<sup>1</sup>, Julien Pansiot<sup>1</sup>, Rahma Hassan-Abdi<sup>1</sup>, Charlie Demene<sup>3</sup>, Marina Colella<sup>1</sup>, Christiane Charriaut-Marlangue<sup>1</sup>, Aline Rideau Batista Novais<sup>1</sup>, Mickael Tanter<sup>3</sup>, Stefania Maccari<sup>4</sup>, Pierre Gressens<sup>1, 5</sup>, Daniel Vaiman<sup>5, 6</sup>, Nadia Soussi-Yanikostas<sup>1\*</sup>, Olivier Baud<sup>1, 2, 5\*</sup>

<sup>1</sup> PROTECT, Inserm U1141, Université Paris Diderot, Sorbonne Paris Cité, Paris, France.

<sup>2</sup> Division of Neonatology and Pediatric Intensive Care, Children's University Hospital of Geneva and University of Geneva, Geneva, Switzerland.

<sup>3</sup> Institut Langevin, CNRS UMR 7587, Inserm U979, ESPCI Paris, PSL Research University, 75005 Paris, France.

<sup>4</sup> University Lille 1, CNRS UMR 8576, 59000 Lille, France; IRCCS Neuromed and Sapienza University of Rome, 00185 Rome, Italy.

<sup>5</sup> PremUP Foundation, 75014, Paris, France.

<sup>6</sup> Institut Cochin, Inserm U1016, UMR8104 CNRS, 75014 Paris, France.

\* Olivier Baud and Nadia Soussi-Yanikostas contributed equally to the work.

### **Corresponding author:**

Prof. Olivier BAUD, Division of Neonatology, Department of Pediatrics, University hospitals, Geneva, Switzerland.

Tel : +41 795534204

Email: [olivier.baud@hcuge.ch](mailto:olivier.baud@hcuge.ch)

## **Funding**

This work was supported by Institut National de la Santé et de la Recherche Médicale (Inserm), Paris-Diderot University, National Center for Scientific Research (CNRS), the French National Research Agency (ANR-16-CE18-0010, ANR-14050HH), the European Research Council under the ERC Advanced grant (339244-FUSIMAGINE), and Fondation NRJ (Institut de France), Fondation PremUP and Fondation Paralysie Cérébrale.

Raw data reported in the manuscript have been located in EMBL-European Bioinformatics Institute (EBI) YYYYYY, created xxxx 2018.

**Acknowledgment:** We thank Francesca Peri (EMBL, Heidelberg, Germany) for providing the Tg(ApoE:GFP) transgenic line. We thank Audrey Toulotte-Aebi for editing the manuscript.

**Conflict of interest:** None of the authors declare no conflict of interest.

## **Abstract**

Prematurity and fetal growth restriction are frequent conditions associated with adverse neurocognitive outcomes. As putative mechanism linking these events and abnormal trajectory of the developing brain, we have previously correlated deregulation of genes controlling neuroinflammation with abnormal brain function and structure. Here, we showed that oxytocin system, impaired by stress-associated perinatal conditions could be rescued by carbetocin, a long-lasting oxytocin receptor agonist. When given early after birth, carbetocin alleviates microglial activation at both transcriptomic and cellular levels, and provides long-term neuroprotection. Targeting oxytocin signaling in the developing brain may be an effective approach to prevent brain damage of perinatal origin.

## Introduction

Neurocognitive disabilities of perinatal origin remain a major burden on children, their families and society, underscoring the need to develop preventive strategies <sup>1 2</sup>. Prematurity and fetal growth restriction (FGR), affecting 15-20% of all pregnancies, are the two leading causes of these learning disabilities and developmental behavioral disorders <sup>3-8</sup>, in both industrialized and developing countries.

Inflammation in the central nervous system plays a key role in the pathophysiology of perinatal brain damage observed in both animal models and human neonates <sup>9</sup>. Although the mechanisms involved in inflammation-induced early brain injury remain unclear, recent evidence has shown that abnormal microglial activation can contribute to white matter damage and alteration of neural circuitry, leading to neurocognitive disabilities and neuropsychiatric disorders in children and adults <sup>10,11</sup>. These findings have been documented not only in models inducing neuroinflammation in neonatal animals <sup>12,13</sup> but also in rat pups subjected to FGR, where an extensive deregulation of genes controlling neuroinflammation in microglial cells has been recently reported <sup>14</sup>. Therefore, the regulation of neuroinflammation early in life therefore offers a relevant approach to neuroprotection.

In addition to inflammation, perinatal stress associated with prematurity or FGR has been associated with disturbances in the Hypothalamic–pituitary–adrenal (HPA) axis and the oxytocin systems with a reduced expression of the hormone oxytocin (OXT) in the hypothalamic paraventricular nucleus <sup>15-17</sup>. Oxytocin, well known for its perinatal function on the uterus and mammary gland, can facilitate a variety of social activities ranging from pair bonding to maternal behavior, which can be impaired by unexpected perinatal events, including prematurity<sup>18</sup>. This hormone is also crucial for normal brain development as demonstrated by its ability to modulate the function of GABA neurons, and by is involved in autistic-like behavior in adulthood <sup>19,20</sup>. In addition to this effects oxytocin exert a protective action in injury condition. Indeed, several reports have showed that OXT alleviates tissue damage in a variety of animal models of injury in the adult brain and heart <sup>21</sup>. Finally, OXT

has peripheral and central anti-inflammatory effects *in vivo* and *in vitro*<sup>22,23</sup>, but little is known about its impact on the developing brain.

Here, we hypothesized that OXT could influence microglial activation in response to perinatal brain injury, and mitigate ensuing damage. To address this issue, we first investigated a double hit insult model in the rat to recapitulate the most frequent perinatal injury affecting the human brain. We further studied OXT effect using this rodent model and a zebrafish model of microglia activation. We report on a set of *in vivo* and *in vitro* studies showing that carbetocin, a long-lasting OXT receptor (OXTR) agonist, when given early in life, regulates microglial activation at both transcriptomic and cellular levels, and provides long-term neuroprotection.

## Results

### Microglial genomic deregulations in response to a double-hit model of perinatal brain injury

We first refined a rat model based on a gestational low protein diet to induce FGR<sup>14</sup>, to improve its clinical relevance. In addition to FGR, a second hit induced by postnatal low-dose IL1 $\beta$  injections to mimic pro-inflammatory events commonly observed in growth-restricted neonates admitted to neonatal intensive care units and associated with subsequent neurocognitive impairments<sup>24</sup> (Fig. 1a). In this double-hit model, early imbalance towards excessive HPA-related hormones (arginine vasopressive (AVP) and corticotropin-releasing hormone (CRH)) and lower expression of OXT was observed in the hypothalamus (Fig. 1b). Cortical brain injury induced upregulation of several genes encoding for pro-inflammatory cytokines on P2 and P4 and disruption of oligodendroglial lineage leading to defective myelination on P10. No gender-related vulnerability to brain damage has been observed in this model.

We next analyzed the transcriptomic effects of the treatment on microglial cells sorted from P4 rat pups. Through Arraymining analysis, we revealed that the low-dose IL1 $\beta$  treatment did not trigger obvious effects on gene expression *versus* controls (Fig. 1c). In contrast, a synergistic effect of the double-hit (antenatal LPD plus postnatal IL1 $\beta$ ) was observed inducing strong modifications of mRNA levels, for both up- and down-regulated genes (Fig. 1c-1e) especially in up-regulated gene sets related to inflammation. Indeed, using a threshold for significance above 1.5-fold change, the numbers of genes induced or repressed compared to controls were found to be much higher in the microglial cells sorted from animals subjected to the double-hit (41 up and 387 down) than in either LPD alone (2 and 123) or IL1 $\beta$  alone (4 and 0) (Fig. 1e). Gene Set Enrichment Analysis (GSEA; <http://software.broadinstitute.org/gsea/index.jsp>)<sup>25</sup> was used to match these genes to gene sets of the “hallmarks” and the “CGP” (Chemical and Genetic Perturbations) databases, encompassing respectively 50 and 3409 gene sets. Analyses revealed an enrichment of

several "hallmark" gene sets involved in the inflammatory response, in line with the immunohistological results (Fig. 1f). Microarray analysis was validated using qRT-PCR on 12 genes showing a close correlation between the two methods of gene expression analysis with a  $r^2=0.8564$  (Supplementary Fig. 1).

Then, transcriptomic data was studied for upregulated genes in response to double hit insult using the network analysis tool Cytoscape (<http://www.cytoscape.org/>), after generating a network using String (<http://string-db.org/>) (Fig. 1f-1h). The network obtained was then simplified by selecting "hub" genes, defined as genes known to be connected to several others. With these tools, we could evaluate the gene-gene interaction network, which showed that the expected number of "edges" (gene-gene relations) was strongly enriched (128 edges found while 43 were expected;  $p$ -value  $< 10^{-100}$ ). Enriched biological processes, cellular components and KEGG pathways are shown in Supplementary Table 1. Within biological processes, activation of immune signaling appeared almost exclusive (Fig. 1g). The network analysis was centered around IL1 $\beta$  which appeared as the major hub gene in the network (Fig. 1h).

Together these data reveal strong evidences that the double-hit model used in this study to mimic perinatal brain injury was associated with an exacerbation of microglial activation such as the induction of the gene *Iba1*, encoding the AIF1 factor, a major factor for microglial activation cascades in parallel with the down-regulation of OXT system in the hypothalamus.

### ***In vivo* effect of carbetocin on microglial activation in rat pups subjected to double hit insult**

Because OXT is a key hormone in several animal models of perinatal stress, and because OXT expression has been found to be significantly reduced in response to LP, we tested the hypothesis that OXT insufficiency was involved in perinatal brain damages observed in our model. We used carbetocin, a long-lasting brain-permeable OXTR agonist <sup>26</sup> injected intraperitoneally (ip) simultaneously with low-dose IL1 $\beta$  on P1 and P2. Double-hit insult induced a protracted growth restriction in rat pups, and this effect on body weight was not modified by

the carbetocin treatment (Supplementary Fig. 2). Microglial activation in response to carbetocin induced a significant reduction of Iba1<sup>+</sup> microglial cells density within the developing white matter in P4 treated animals (Fig. 2a, b). Using qRT-PCR on microglial cells sorted from P4 rat pups, we found that carbetocin was associated with no detectable effect on gene expression of several M1 and M2 markers of microglial reactivity in control animals. In contrast, carbetocin significantly prevented up-regulation of IL6, IL1 $\beta$ , TNF $\alpha$  and iNOS, all M1 markers, in animals subjected to double-hit insult (Fig. 2c). Conversely, carbetocin did not change gene expression of M2 markers including Arg1, IGF1, Mrc1 and Sphk1, in either controls or LPD+IL1 $\beta$  animals. Focusing on the effects of carbetocin at the transcriptomic levels, microarray analysis revealed a 50% reduction in the number of genes up-regulated more than 1.5 fold (16 vs 32) in microglial cells sorted from animals treated with carbetocin compared to untreated animals (Fig. 2d, e). The networks obtained using String and Cytoscape softwares on gene expression of the microglial cells isolated from animals treated by carbetocin, included genes involved in the induction or regulation of brain inflammation including IL10, CXCL2, NOS2 and NCAM1 (Fig. 2f). Interestingly, the main gene sets involved in inflammatory response and composed of up-regulated genes in the double hit model were found systematically, in the gene sets down-regulated by carbetocin treatment (Fig. 2g). Looking at the “TNF $\alpha$  signaling via NF $\kappa$ B cascade” gene set in more details, we isolated the subset of core genes (involved in the enrichment score calculation) composed of 57 genes that were up-regulated in LPD+IL1 $\beta$  animals and found down-regulated by carbetocin treatment. The average induction was estimated at 1.41-fold, while carbetocin treatment resulted in a reduction at 0.81-fold. The product of the inductions for each gene yielded an induction ratio of 1.14, which was not significantly different from 1 (Fig. 2h). Together these findings demonstrated that carbetocin treatment restores a control profile of microglial gene expression in animals subjected to double-hit challenge.

### **Effect of carbetocin on FGR-associated microglial activation *in vitro***

To further investigate the direct effect of carbetocin on microglial activation *in vitro*, we studied cell morphology and expression of genes related to microglial phenotypes (classic and alternative activation) in microglial cells sorted at P2 from animals subjected to LPD and controls, with and without pro-inflammatory exposure to IL1 $\beta$ +INF $\gamma$  for 9h. Forty eight hours after sorting and plating, pure microglial cell cultures were stained using Iba1 antibody (Fig. 3a). Cell morphology was significantly different in cells sorted from LPD animals compared to the controls, with a reduced cell surface area, a lower proportion of cells with an area above 45 $\mu\text{m}^2$ , a reduced cell perimeter and increased cell circularity, a marker of amoeboid shape of the cells (Fig. 3b, c). Multiplex assay method (Luminex xMAP<sup>®</sup>) for cytokine concentration measurements in the culture medium of primary microglia sorted from LPD-exposed animals revealed a marked increase in concentrations of several pro-inflammatory cytokines compared to control animals (Supplementary Fig. 3). Pro-inflammatory challenge induced cell morphology changes towards amoeboid shape in control cells but not in FGR-derived cells which were already activated. In both cell groups, carbetocin was able to significantly reverse microglial activation assessed on cell size, distribution of cell size (Fig 3c, d), cell perimeter and circularity. Gene expressions of three microglial markers of classic activation (M1: TNF $\alpha$ , IL6, iNOS) and one marker of alternative activation (M2: Mannose Receptor C 1, Mrc1) were assessed in primary microglial cultured cells sorted from LPD brains and controls under basal conditions and after IL1 $\beta$ +INF $\gamma$  stimulation in the presence or absence of carbetocin alone or in combination with OXTR antagonist L-368-899 (Fig. 3e). A 4-fold increase in the expression of all M1 markers, but not Mrc1, was detected in microglial cells from LPD brain both under basal conditions and after stimulation. Carbetocin was able to partially prevent microglial over-activation in response to pro-inflammatory stimulus, more notably in microglial cells sorted from LPD-exposed animals. L-368-899 significantly reversed this effect suggesting that carbetocin effect on microglial activation *in vitro* was OXTR-mediated.

## **Effect of carbetocin on hydrocortisone-induced microglia activation in zebrafish embryos**

We further investigate further the effect of carbetocin on microglia activation *in vivo*, using an established model of neuroinflammation induced by chronic hydrocortisone incubation of zebrafish larvae <sup>27</sup>, applied on the Tg[ApoE:eGFP] transgenic line <sup>28</sup>, which allows live imaging of microglial cells in a physiological situation (Fig. 4a). Previous works had shown that during zebrafish development, microglial cells enter the brain from 35 hours post-fertilization (hpf) onward and fully colonized the optic tectum by 60 hpf (Fig. 4b, c). Lastly, from 72 hpf onward, microglial cells displayed a highly ramified morphology, and expressed differentiation markers including apolipoprotein E (apoE), suggestive of fully differentiated states <sup>29</sup>.

First, we studied the molecular and cellular microglia phenotypes induced by sustained hydrocortisone incubation. Quantitative RT-PCR analysis indicated that zebrafish embryos treated from 1 hpf to 7 days post-fertilization (dpf) with 1.3  $\mu$ M hydrocortisone, displayed a significant 3- to 6.7-fold increased expression of the pro-inflammatory cytokines IL1 $\beta$ , IL8 and TNF $\alpha$  (Fig. 4d). Importantly, live imaging showed that whereas hydrocortisone treatment did not induce any visible morphological defect in zebrafish larvae, it caused dramatic changes in the shape of microglial cells: we observed a striking fall in the number and length of cell processes, with microglial cells showing a more amoeboid shape and much fewer processes, when compared to untreated controls (Fig. 4e). Next, we analyzed the effects of a 2-day treatment with 1  $\mu$ M carbetocin, on 6 and 7 dpf zebrafish embryos, which have been previously treated with 1.3  $\mu$ M hydrocortisone, or untreated (Fig. 4a). First, qRT-PCR analysis indicated that while carbetocin alone did not modify cytokine expression, it markedly attenuated the increased expression of pro-inflammatory cytokines induced by hydrocortisone administration (Fig. 4d). In addition, live imaging showed that carbetocin alone did not induce any detectable change of the morphology of microglial cells. In contrast, in embryos that have been previously treated with hydrocortisone, a 2-day treatment with carbetocin markedly attenuate the cell shape changes induced by hydrocortisone, with

microglial cells recovering elongated processes and a ramified morphology, similar to that seen in non-treated controls (Fig. 4e). The effect of treatments (hydrocortisone +/- carbetocin) on microglia morphology was studied using Imaris software (Bitplane Inc.), which allows the precise measurement of different cell variables, such as sphericity, volume, surface area and surface area/volume ratio. Imaris analysis confirmed that hydrocortisone treatment markedly modified the morphology of microglial cells as shown by the significant increase of their sphericity combined with marked decreases of their volume, surface area, and surface area/volume ratio (Fig. 4f). Although carbetocin alone did not induce any detectable change in the morphology of microglial cells, it significantly reversed the effect of hydrocortisone (Fig. 4f). Together, these data are strong evidence that carbetocin is able to mitigate microglia activation in zebrafish.

To further characterize the behavior and dynamics of microglial cells in response to hydrocortisone +/- carbetocin, we performed *in vivo* time-lapse confocal imaging combined with image analysis and quantification using the Imaris software (Bitplane Inc.) (Fig. 4g and Supplementary videos 1, 2, 3 and 4). Results showed that hydrocortisone treatment induced significant changes in microglial dynamics including a significant increase in the mean speed of their processes and mean track displacement measurements (Fig. 4g-i). In addition, although carbetocin alone had no effect on the dynamics of microglial cells or that of their processes, it fully countered the effects of hydrocortisone, resulting in quantitative measurements similar to those in control non-treated embryos.

### **Long-term impact of carbetocin on myelination, *in vivo* brain connectivity and long-term behavior**

Excessive microglial activation has been found to play a key role in defective myelination and neurocognitive impairments in both pre-clinical models of perinatal brain damages and humans <sup>10</sup>. We therefore investigated whether carbetocin, by targeting neuroinflammation, could prevent brain damages and its long-term consequences in the present model of perinatal brain injury. Despite no detectable gross morphological damage of the brain

following double-hit insult, assessment of myelination at P10 revealed a significant decrease in the myelin content (MBP<sup>+</sup> fibers) and APC<sup>+</sup> mature oligodendrocytes within the cingulate white matter and external capsule in animals subjected to LPD+IL1 $\beta$  challenge (Supplementary Fig 4, Fig. 5a). The total oligodendroglial population (Olig2<sup>+</sup> cells) was found to be unaffected suggesting a disruption of the oligodendroglial lineage as previously reported in other models of inflammatory-induced white matter lesions <sup>12</sup>. fUS imaging consists in the repetition every two seconds of the acquisition of Ultrafast Doppler movies lasting 0.5 second (Supplementary Fig. 5a, b), enabling the computation of highly sensitive cerebral blood volume (CBV) maps. By doing so, spontaneous fluctuations of CBV related to underlying neuronal activity were recorded by fUS in a coronal imaging plane during two successive 10-min periods of resting state in animals at P28. Each brain imaging plane was co-registered with a rat brain atlas reference (Paxinos & Watson, 6<sup>th</sup> Ed., 2007) delineating 10 functional regions of interest (ROIs) per hemisphere (Supplementary Fig. 5c) in order to compute average ROIs-based CBV signals that exhibit various degrees of correlation, the latter reflecting the underlying cerebral connectivity between ROIs (Supplementary Fig. 5d). Pearson correlation coefficients between inter and intra-hemispheric couples of ROIs were gathered into a matrix which correlation levels and spatial pattern reflected a degree of cerebral connectivity that can be compared between groups (Supplementary Fig. 5e). Complete correlation matrices are displayed for qualitative visual pattern difference (Fig. 5b), and quantification and statistical difference were evaluated for interhemispheric (anti-diagonal coefficients) and intra-hemispheric (first off-diagonal coefficients) connectivity. Interhemispheric somatosensory connectivity was significantly depressed in animals exposed to perinatal brain injury in the retrosplenial granular cortex (RSG), in a critical position between the hippocampal formation and the neocortex retrosplenial dysgranular cortex (RSD), medial and lateral parietal association cortex (LPtA, MPtA) and in the most of parts of the thalamic area (Thal D, Thal V and Thal M) (Fig. 5c). Carbetocin treatment prevented the loss of inter-hemispheric connectivity in all cases except medial thalamus (Thal M). Intrahemispheric connectivity was also found to be severely impaired mostly within

neocortex retrosplenial cortices, between neocortex retrosplenial cortex and parietal association cortices, and between the ventral and dorsal thalamus (Fig. 5d). Again, early carbetocin given during the neonatal period was associated with a significant prevention of most of these long-term functional disorders involving RSD and the parietal association cortex.

Finally, behavioral consequences of LPD+IL1 $\beta$  exposure and carbetocin treatment were assessed in 28-day animals for open-field (OF) and 2-month animals for Y-maze tests. Track records in the OF were divided into three different zones from center to periphery of the arena (Fig. 6a, b). Distance traveled in the each area, cumulative time duration spent in each and velocity were quantified. Animals subjected to LPD+IL1 $\beta$  spent significantly more time in the periphery of the arena than did control animals. They traveled a longer distance in the intermediate zone between the periphery and the center of the arena and their velocity was found higher in the center but not in the periphery, findings suggesting anxiety-like behavior (Fig. 6b). Carbetocin treatment fully prevented these behavioral anomalies. In the Y-maze test, distance traveled during the first 5 minutes of the habituation period (during which only two arms of the Y-maze are available) was found significantly greater in animals subjected to the double-hit than in controls (Fig. 6c). Percentage of time spent in the novel arm during the retention task of the Y-maze was found significantly lower in LPD+IL1 $\beta$  animals (Fig. 6d). Percentage of time spent in the novel arm during the retention task of the Y-maze was found significantly lower in LPD+IL1 $\beta$  animals, suggesting their incapacity to recognize novelty. These effects were consistently prevented by carbetocin treatment.

## Discussion

This study demonstrates that the early postnatal activation of OXTR after birth is able to modulate microglial activity, and is associated with a significant protection of the neonatal brain subjected to pro-inflammatory challenge. Carbetocin reduced most of the effects, in particular microglial activation, induced in a double hit model of perinatal brain injury induced by gestational LPD and potentiated by postnatal injections of subliminal doses of IL1 $\beta$ . The central anti-inflammatory effects of carbetocin have been revealed *in vivo* in rat pups and reproduced both *in vitro* on stimulated primary microglial cell culture sorted from rats subjected to LPD and *in vivo* in a zebrafish model of early-life neuro-inflammation. These findings were associated with *in vivo* effects on myelination, and on long-term brain connectivity and behavior.

The present animal model was designed to be as relevant as possible considering the complexity of FGR. In humans, FGR significantly increases rates of stillbirth, neonatal mortality and morbidity responsible for considerable lifetime costs<sup>30</sup>. Currently the FGR rate is the highest in over 20 years, and is likely to rise further owing to the increasing rates of infertility treatments, multiple pregnancies, professional workloads and older mothers, as well as prenatal exposure to stress, nicotine and malnutrition<sup>31</sup>. Following birth, growth-restricted neonates are more prone to develop subsequent inflammatory-related damage resulting in cerebral palsy, cognitive and behavioral disorders<sup>32</sup>. The preclinical model used in the present study was set up to replicate both growth restriction and inflammatory-related events frequently observed following FGR in human neonates. Recent findings have suggested that growth-restricted rats already show an exacerbated neuro-inflammatory response associated with damages to the developing brain<sup>14,33</sup>. Like in humans, this animal model was found to induce multi-organ morbidities involving, in addition to the brain, the developing lungs<sup>34</sup> and kidneys<sup>35</sup>. In this vulnerable context, subliminal inflammatory challenge had a synergistic deleterious effect in growth-restricted rat pups.

Like many other models of perinatal stress, our model was found to be associated with an early imbalance between the HPA axis and the OXT system, two hypothalamic systems of crucial importance during brain development: exposure to a series of unpredictable stresses during the final week of pregnancy <sup>15</sup>, repeated restraint stress <sup>36</sup> or prenatal cocaine <sup>37</sup> induced in the offspring an elevation of CRH production concomitantly with a reduced OXT levels in the hypothalamus. The role of this imbalance in the developmental programming of neuro-inflammation remains to be clarified. As a first hypothesis, decreased OXT system activity and the resulting increased HPA axis activity could result in an early excessive exposure to glucocorticoids that could, by epigenetic mechanisms, permanently decrease the expression of glucocorticoid receptor (GR) in immune cells including microglial cells. As a result, this enduring loss of anti-inflammatory effects of endogenous glucocorticoids can shift the immune response toward a pro-inflammatory phenotype later in life <sup>38,39</sup>.

Here we have demonstrated that the long-lasting oxytocin receptor agonist, carbetocin was able to block the microglial activation associated with gestational LPD, not only *in vivo* but also directly *in vitro*. Similar anti-inflammatory effects of OXT have previously been reported. Oxytocin has been shown to reduce the neuroendocrine and cytokine response to bacterial endotoxin in adults <sup>40</sup>. Protective effects of OXT during cardiac or renal ischemia in rats were also found to be associated with decreased levels of circulating pro-inflammatory cytokines <sup>41</sup> <sup>42</sup>. Moreover, OXT inhibits LPS-stimulated pro-inflammatory cytokine expression in macrophages and endothelial cells <sup>43</sup> and even in microglial cells <sup>22</sup>. The biological action of OTX is linked to the activation of OTXR, a selective seven-transmembrane G<sub>q</sub>/G<sub>i</sub>-coupled receptor expressed both in astrocytes and in microglia <sup>21,22</sup>, particularly in response to inflammation <sup>44</sup>. Indeed, exposure of microglia cells to inflammatory stimulus induced a time-dependent increase in OTXR expression suggesting that the OTX system is an inducible system that undergoes a dynamic regulation in response to immune challenge.

The molecular basis of the neuroprotective action of OTX remains unclear, and modulation of the downstream ERK/MAPK pathway in microglial cells has been reported in only one study

<sup>22</sup>. Alternative pathways could also be involved including other molecular effectors of OTXR (e.g. NF $\kappa$ B, eEF2 eukaryotic elongation factor 2) and could be linked to the modulation of the expression of other neurotransmitter receptors on microglial surface membrane <sup>45</sup>. The gene expression profile corrected by carbetocin treatment concerns genes involved in many different stresses, including DNA damage and apoptosis (Gadd45a), angiogenesis and coagulation (Vegfa, F3), inflammation (Rel, RelB, NF $\kappa$ B, IL1 $\beta$ ). This concerted action could explain the various and sustained improvements observed in the treated animals.

Interestingly, our findings were not restricted to rodents, but were replicated in zebrafish embryos. Indeed, by using the optically transparent zebrafish embryo where the microglial cells are fluorescent, combined to carbetocin treatment that have been beforehand subjected to pro-inflammatory hydrocortisone, we have shown a dramatic modulation of the dynamics of microglial cell processes, deep remodeling of microglia morphology and changes in cytokine gene regulation and expression. Altogether, these data demonstrate an evolutionarily conserved anti-inflammatory function of OXT-OXTR, which targets the microglia and markedly alleviates the differentiation of these cells exposed to hydrocortisone towards an activated M1-like profile.

Targeting neuro-inflammation is critical in protecting the developing brain because both systemic and central inflammation play a role in the blockade of oligodendrocyte maturation leading to long-term myelination defects, and finally cognitive defects in the neonate <sup>46</sup>. In neonates born after FGR, the levels of circulating cytokines were found to be significantly increased on days 7 and 14 compared with levels measured in neonates without FGR <sup>24,47</sup>. This postnatal systemic pro-inflammatory state following FGR could, at least in part, be responsible for the brain insults and neurodevelopmental impairments detected in childhood in these individuals. At the core of the vulnerability of the immature brain lies the systemic up-regulation of pro-inflammatory cytokines also leading to diffuse activation of cerebral microglia <sup>48</sup>.

Microglia cells play a major role in the vulnerability of the immature brain to various challenges, but microglia mediates not only classic cytotoxicity but also alternative functions

including repair, regeneration and immunosuppression, owing to their ability to acquire diverse activation states or phenotypes <sup>49</sup>. Their exacerbated activation may reverse their beneficial physiological properties, impairing neurogenesis and myelination and leading to neuronal and axonal death <sup>50</sup>. Some microglia functions have been shown to be required for myelination: an excessive microglial activation is usually associated with a reduction in oligodendrocyte progenitors, with a maturational arrest of the oligodendroglial lineage and with hypo-myelination <sup>12,51</sup>.

Although excessive microglial activation is linked to injury, microglial depletion is also associated with adverse effects in the developing brain <sup>52,53</sup>. The colonization of the human brain by microglial cells during fetal life, between 12 and 24 GW, leads to clusters of activated microglia in the corpus callosum, in the axonal crossroads and in the periventricular white matter, all areas usually injured in neonates <sup>54</sup>. FGR, which usually occurs at 18-24 GW and during the third trimester, could have a strong impact on the microglial cell lineage during this critical period. Some mouse models of genetic disruptions of microglial IL18 <sup>55</sup> or of galectin 3, interfering with the pro-inflammatory response <sup>56</sup>, suggest that a finely tuned modulation of microglial activation through specific pathways (i.e. OXTR activation) rather than its global inhibition should be considered as an important therapeutic target to protect the developing brain.

Anti-inflammatory effects of carbetocin are probably responsible for the protection against the consequences of LPD+IL1 $\beta$  on myelination, seen not only at histological level but also at a functional level as evidenced by functional ultrasound imaging (fUS) and behavioral testing. We have already reported the high sensitivity of fUS technology not only in rodents <sup>14</sup> but also in human neonates <sup>57</sup>. fUS offers a valuable combination of penetration and spatiotemporal resolution unique for translational studies and appears to be a promising novel brain imaging modality in the field of perinatal medicine <sup>57</sup>. In addition, screening high-risk neonates through novel markers of brain function, developed and assessed in preclinical models of brain damage, would have significant benefits in improving knowledge on

functional prognosis and in identifying infants who could benefit from neuroprotective strategies to be tested in forthcoming clinical trials <sup>58</sup>.

Here, long-term alterations in brain connectivity in response to LPD+IL1 $\beta$  challenge and the beneficial effect of early carbetocin treatment were associated with changes in with anxiety-like behavior in the open-field test and cognitive abilities in the Y-maze test. In another model of growth-restricted rabbits, microstructural changes in gray matter, decreased connectivity, more anxiety, and memory problems had previously been reported <sup>59</sup>. Interestingly, in human children born growth-restricted, altered patterns of brain connectivity have also been correlated with motor, cognitive and behavioral outcomes <sup>60</sup>.

In addition to structural damages, neuroinflammation is a common feature in the development of many neuropsychiatric diseases including autistic spectrum disorders (ASD), depressives and psychotics syndromes, and Alzheimer disease <sup>61,62</sup>. Most of these disorders may originate in the perinatal life through exposure to stress, trauma and/or inflammation in the Developmental Origins of Health and Disease (DOHaD) framework, all of which have the ability to program individuals for an enduring constitutive vulnerability to central inflammatory responses <sup>63</sup>. Based on the present study, we speculate that reduced OXT tonus provoked by LPD+IL1 $\beta$  exposure could be a starting point for a pro-inflammatory trajectory leading to an increased vulnerability regarding future neuropsychiatric disorders, a frequent co-morbidity in infants born preterm or following FGR. Restoring central OXT tonus early in life could be beneficial on neurobehavioral outcomes in these infants exposed to perinatal inflammation. An early postnatal OXT treatment has been shown to prevent social and learning deficits in *Magel2*<sup>-/-</sup> adult mice (Prader-Willi syndrome) and ASD <sup>64</sup> and a causal link between OXT and social behavior in a mouse model of ASD has already been reported <sup>65</sup>.

In conclusion, our findings reveal that modulation of activated microglia by carbetocin, a long-lasting brain permeant OXTR agonist, confers neuroprotection of the immature brain towards perinatal insult. These findings suggest a key role of the OXT system as a promising

therapeutic pathway in preventing deleterious effects of perinatal stress associated with preterm birth or fetal growth restriction.

## Figure legends

### **Fig. 1. The double-hit rat model associating gestational low protein diet with postnatal inflammatory challenge.**

**a.** Pups from isocaloric low protein diet (LPD, 9% protein) and normal diet (Ctl, 22% protein) fed mothers were injected i.p. at postnatal (P) days 1 and 2 twice a day with IL1 $\beta$ . Brain were then analyzed for mRNA transcription and protein expression directly or after microglia magnetic cell sorting. **b.** Consequences of the LPD treatment on the hypothalamic HPA and oxytocin systems mRNA expression at P1, and of LPD+IL1 $\beta$  treatment on the cortical mRNA at P2 and P4 (open circle) and on cortical protein expression at P4 and P10 (full circle). Data are means  $\pm$  SEM. All data were found significant and two-tailed unpaired t-test was used for comparisons (See Supplementary Table 5 for detailed numbers, t- and p-values). **c.** Arraymining analysis performed on sorted microglial cells at P4. **d. e.** Effects of LPD over control, and strong synergistic effect when the LPD and IL1 $\beta$  treatments are applied together (N=3 sample per group). **f.** Clustering focused on the comparison between microglial transcripts from LPD+IL1 $\beta$  and controls. **g.** GSEA analysis of the differential hallmarks of up-regulated genes in the comparison LPD+IL1 $\beta$  vs Controls. Significantly enriched gene clusters linked to inflammatory responses appeared in the up-regulated genes. **h.** Up-regulated genes network on LPD and IL1 $\beta$  treatment. The blue color is more intense for the most abundant transcripts.

### **Fig. 2. Central anti-inflammatory action of early postnatal carbetocin treatment *in vivo*.**

**a.** Representative photomicrographs of Iba1<sup>+</sup> cells (red) within cortical the white matter of P4 rat pups in the 4 experimental groups. Bars=100  $\mu$ m; LV: lateral ventricle. **b.** Carbetocin restores the number of Iba1<sup>+</sup> ameboid cells per slice within in the white matter of LPD+IL1 $\beta$  animals. **c.** Pro-inflammatory (M1) and anti-inflammatory or immuno-modulatory (M2) mRNA cortical expression at P1-P2 in in the 4 experimental groups. All comparisons in **b** and **c** were performed using one-way ANOVA followed by Newman-Keuls multiple comparison tests

when appropriate. Comparisons were performed using one-way ANOVA followed by Newman-Keuls multiple comparison tests; \* and \$ is respect to control and LPD+IL1 $\beta$  respectively. Data are means  $\pm$  SEM. (See Supplementary Table 5 for detailed numbers, F- and p-values). **d.** Microarray analysis of microglia sorted cells reveals a clear clustering in gene expression between LPD+IL1 $\beta$  and LPD+IL1 $\beta$ +carbetocin (N=3 per group). **e.** Venn diagram for up- and down-regulated genes in microglia from LPD+IL1 $\beta$  and LPD+IL1 $\beta$ +carbetocin respect to control. **f.** Up- and down-regulated genes network in LPD+IL1 $\beta$  with carbetocin treatment. **g.** GSEA analysis revealed that differential hallmarks gene sets of up-regulated genes by LPD+IL1 $\beta$  challenge, are systematically enriched in down regulated genes by carbetocin treatment. **h.** Example of gene sets up-regulated by LPD+IL1 $\beta$  treatment, and corrected by carbetocin treatment (TNF $\alpha$  signaling via NF $\kappa$ B). Gene expression ratios of core-induced genes were collected. In samples from carbetocin treated-animals, 57 genes of the core were down-regulated. The global outcome tends to bring back the genes to a ratio of 1.

**Fig. 3. *In vitro* effects of carbetocin and OXTR antagonist in primary microglial cultured cells sorted from control and LPD brains with and without pro-inflammatory stimulation.**

**a.** Representative photomicrographs of primary culture of microglial cells sorted from control and LPD brains at P2. Microglial cells were stained with Iba1 in basal condition, after pro-inflammatory stimulation (IL1 $\beta$  + INF $\gamma$ ) in presence or not of 1 $\mu$ M carbetocin. Bar= 50 $\mu$ m. **b.** Microglial cell morphological changes induced by IL1 $\beta$ +INF $\gamma$  stimulation in presence or not of carbetocin in control and LPD groups considering cells area, cells perimeter and cells circularity. **c.** Mean cells area, for each condition, in 3 category of cells area with limit of size based on a control microglia in basal condition divided in 3 equal sub-groups. **d.** Distribution of cells number (in percent) for each of the 3 cell size groups for each condition. **e.** Gene expression of microglia phenotypic markers in primary microglial cultured cells sorted from control and LPD brains in basal condition and after IL1 $\beta$ +INF $\gamma$  stimulation in presence or not

of carbetocin alone or in combination with the OXTR antagonist (L-368-899). IL6, TNF $\alpha$ , and iNOS mRNA (two-way ANOVA,  $P < 0.001$  for all) and Mrc1 mRNA (two-way ANOVA,  $P = 1.99$ ). Comparisons were performed using two-way ANOVA followed by Newman-Keuls multiple comparison tests; \*, is respect to basal condition in either Ctl or LPD groups, \$ is respect to IL1 $\beta$ +INF $\gamma$  in either Ctl or LPD groups, # is respect to same condition in LPD compared to the control group, § is respect to L-368-899 compared to carbetocin effect. Data are means  $\pm$  SEM. (See Supplementary Table 5 for detailed numbers, F- and p-values).

**Fig. 4. Carbetocin effect on cortisol-induced microglia activation in zebrafish.**

**a.** Experimental set-up and drug exposure to dechorionated one day-old embryos. **b.** Live imaging of microglial cells in 8 dpf Tg[Apo-E-GFP] embryos, in which microglial cells display an intense green fluorescent labelling used to follow their morphological changes and dynamic behaviour *in vivo*. Anterior is on the right. **c.** Schematic drawing of the optic tectum, region of interest imaged in this study (red square). **d.** Carbetocin markedly decreases expression of cortisone-induced pro-inflammatory cytokines IL1 $\beta$ , TNF $\alpha$ , and IL8. **e.** Carbetocin fully alleviates cortisol-induced shape changes of microglial cells. Scale bars: 50 $\mu$ m. Lower panel depicts representative 3D Imaris software-reconstruction (Bitplane Inc.) of isolated microglial cells for each group. Scale bars: 10 $\mu$ m. **f.** Quantification of microglia cell shape changes in response to the different drugs. Microglial cells of embryos exposed to hydrocortisone showed highly significant morphological changes, fully prevented by carbetocin. Carbetocin alone in control embryos have no detectable effect. **g.** Representative images of microglial cells from Tg[Apo-E-GFP] embryos incubated in E3 medium used for time-lapse analysis. See also supplementary Movies S1 to S4 that show the dynamic behavior of microglial processes. Scale bar: 50 $\mu$ m. **h, i.** Quantification of microglia processes dynamics (process track displacement and process speed) and performed using the Imaris software (Bitplane Inc.). All comparisons were performed using one-way ANOVA followed by Newman-Keuls multiple comparison tests; \*\*\* and \$\$\$ ( $p < 0.001$ ) is respect to control and to

hydrocortisone groups, respectively. Data are means  $\pm$  SEM. (See Supplementary Table 5 for detailed numbers, F- and p-values).

**Fig. 5. Consequences of LPD+IL1 $\beta$  and carbetocin treatment on myelination and functional intrinsic connectivity of the brain.**

**a.** Quantification of MBP, APC and Olig2 immuno-reactivity in response to LPD+IL1 $\beta$  challenge and carbetocin treatment. **b.** Average functional connectivity map in the control and LPD+IL1 $\beta$  animals treated or not with carbetocin. Pearson correlation coefficients are indicated for the right and left hemisphere in the cortex (RSG, retrosplenial granular cortex; RSD, retrosplenial dysgranular cortex; MPtA, medial parietal association cortex; LPtA, lateral parietal association cortex), in the hippocampus (Hippo), in the dorsal, ventral and medial thalamic area (Thal D, Thal V and Thal M, respectively) and in medial and lateral hypothalamic area (Hypot M and Hypot L, respectively). **c.** Loss of inter-hemispheric functional connectivity in LPD+IL1 $\beta$  animals and correction by early carbetocin treatment. For statistical analyses, matrix Pearson coefficients were transformed using a Fisher transformation. Comparisons were performed using one-way ANOVA followed by Newman-Keuls multiple comparison tests; \* and \$ is respect to control and LPD+IL1 $\beta$  respectively. Data are means  $\pm$  SEM. (See Supplementary Table 5 for detailed numbers, F- and p-values).

**Fig. 6. Behavioral consequences of LPD+IL1 $\beta$  and carbetocin treatment in juvenile and adult animals.**

**a.** Representative track records in the open field (OF) test performed in the 4 experimental groups at 2 months of age. **b.** Subdivision of the open field area in three complementary zones defines as periphery (Periph), intermediate (Inter) and center. All comparisons were performed using two-way ANOVA for repeated measures, followed by Bonferroni multiple comparison tests when appropriate, \* is respect to control, \$ respect to LPD+IL1 $\beta$ . Data are means  $\pm$  SEM. (See Supplementary Table 5 for detailed numbers, F- and p-values). **c, d.** Behavior during the acquisition and the retention tasks of the Y-maze. Distance traveled

during the 5 first minutes of the 15 minutes of the Y-maze habituation period during which only two arms of the Y-maze are available (**c**). Percentage of time spent in the novel arm during the retention task of the Y-maze, 3 hours after the acquisition (**d**). Comparisons were performed using one-way ANOVA followed by Newman-Keuls multiple comparison tests; \* and \$ is respect to control and LPD+IL1 $\beta$  respectively. Data are means  $\pm$  SEM. (See Supplementary Table 5 for detailed numbers, F- and p-values).

## Supplementary figure legends

**Supplementary Figure 1: Correlation between microarray analysis and qRT-PCR based on 12 genes.** Data show a close correlation between the two methods of gene expression analysis with a  $r^2=0.8564$ .

**Supplementary Figure 2: Body weight growth from P1 to P28 in the four experimental groups.**

**Supplementary Figure 3: Multiplex assay for cytokine concentration measurements in the culture medium of primary microglia sorted from LPD-exposed and control animals.** Two-tailed unpaired t-test was used for comparisons normalized to controls. \*\*:  $p<0.01$ , \*:  $p<0.05$ . Data are means  $\pm$  SEM.

**Supplementary Figure 4.** Representative photomicrographs of MBP immuno-reactivity assessment in the cingular and lateral white matter (CWM and LWM, respectively) in P10 animals.

**Supplementary Figure 5: Experimental method for the *in vivo* assessment of the brain functional connectivity, measured by fUS imaging during resting state at P28.**

**a.** After a control or LPD+IL1 $\beta$  treatment, associated or not with carbetocin injection, resulting in 4 pup groups (Ctl N=9, Ctl+Carbe N=7, LPD+IL1 $\beta$  N=9, LPD+IL1 $\beta$ +Carbe N=9), connectivity fUS imaging was performed at 28 post-partum days ( $\pm$  2 days). **b.** fUS imaging consist in the 300 repetitions of UfD image acquired every 2s, resulting in 10 minutes of resting state imaging data. These 10 minutes of resting state imaging was performed two times consecutively for each animal. Each UfD image itself consists in the recording during 0.5s of 250 ultrasound images acquired at a framerate of 500Hz, enabling precise discrimination of the blood flow signal. Intensity in one pixel of a UfD image is

therefore proportional to the local blood volume. These images are registered with a functional rat brain atlas for further regions of interest (ROIs) based subdivision. **c.** Based on this registration 10 ROIs are delineated on each side, resulting in a total of 20 ROIs overall. **d.** In each of these regions the UfD signal is spatially averaged and temporally normalized to calculate Pearson correlation coefficient between every couple of signals. In this example, RSD signal is strongly similar on the left and right side (blue and purple signals), resulting in a high correlation coefficient (0.87), whereas correlation is quite weak between left RSD and left ventral thalamus (blue and pink signals)(corr = 0.24), this being interpreted as a low connectivity at that moment between those 2 cerebral structures. **e.** All these correlation coefficients are gathered into a matrix whose levels and spatial patterns reflect a degree of cerebral connectivity that can be compared between groups. This matrix is symmetrical, and one half is displayed as color for qualitative visual inspection and the other half is displayed as numerical values. The coefficients framed in white correspond to the so-called inter-hemispheric connectivity and the coefficients framed in blue correspond to the so-called intra-hemispheric connectivity (that can therefore be assessed on both left and right side).

**Supplementary Figure 6: Time line representing the double hit rat model combining gestational low protein diet (LPD) with postnatal IL1 $\beta$  challenge associated or not with carbetocin treatment and main endpoints assessed in the study.** Pups from LPD fed mothers (isocaloric 9% of protein respect to 22% in control) were used at P2 for the *in-vitro* experiments, CD11B<sup>+</sup> microglia from P2 pups were magnetically sorted (MACS) and cultivated for an *in vitro* pro-inflammatory stimulation (IL1 $\beta$ , 50ng/ml + INF $\gamma$ , 20ng/ml) in presence or not of 1 $\mu$ M carbetocin and/or of the OXTR antagonist (L-368-899, 2 $\mu$ M). For *in vivo* experiments LPD pups were injected ip at postnatal (P) days 1 & 2 (P1 & P2) twice a day with the pro-inflammatory cytokine IL1 $\beta$  (20 $\mu$ g/kg/injection) alone or in combination with the oxytocin receptor agonist, carbetocin (1mg/kg). Four groups were examined (control, control+carbetocin, LPD+IL1 $\beta$  and LPD+IL1 $\beta$ +carbetocin). Cytokines mRNA expression were examined at P2 and P4 on cortex, microarray analysis were

performed on magnetically sorted microglia at P4. Iba1<sup>+</sup> amoeboid microglial cells were stained and counted on brain slice at P4. White matter and oligodendrocyte maturation were examined by immunohistochemistry at P10. Transcranial Ultrafast Doppler was used for assessing cerebral connectivity at P28  $\pm$  2 days. And finally, anxiety-like behavior was observed at P28 in the open field test and spatial memory performance was assessed in the Y-maze on 2-month-old animals.

**Supplementary video S1-S4.**

Movies of microglial cells from Tg[ApoE:GFP] embryos incubated in E3 medium alone (Ctl) or treated with hydrocortisone (1.3  $\mu$ M) or carbetocin (1  $\mu$ M, Carbe) alone or in combination (Hydrocortisone+Carbe), showing the dynamic behaviour of microglia and their filopodes.

## References

1. Katz, J., *et al.* Mortality risk in preterm and small-for-gestational-age infants in low-income and middle-income countries: a pooled country analysis. *Lancet* **382**, 417-425 (2013).
2. Christensen, D., *et al.* Prevalence of cerebral palsy, co-occurring autism spectrum disorders, and motor functioning - Autism and Developmental Disabilities Monitoring Network, USA, 2008. *Dev Med Child Neurol* **56**, 59-65 (2014).
3. Jarvis, S., *et al.* Cerebral palsy and intrauterine growth in single births: European collaborative study. *Lancet* **362**, 1106-1111 (2003).
4. Guellec, I., *et al.* Neurologic outcomes at school age in very preterm infants born with severe or mild growth restriction. *Pediatrics* **127**, e883-891 (2011).
5. Strang-Karlsson, S., *et al.* Very low birth weight and behavioral symptoms of attention deficit hyperactivity disorder in young adulthood: the Helsinki study of very-low-birth-weight adults. *Am J Psychiatry* **165**, 1345-1353 (2008).
6. Hack, M., *et al.* Outcomes in young adulthood for very-low-birth-weight infants. *N Engl J Med* **346**, 149-157 (2002).
7. Wiles, N.J., *et al.* Fetal growth and childhood behavioral problems: results from the ALSPAC cohort. *Am J Epidemiol* **163**, 829-837 (2006).
8. Geva, R., Eshel, R., Leitner, Y., Fattal-Valevski, A. & Harel, S. Memory functions of children born with asymmetric intrauterine growth restriction. *Brain Res* **1117**, 186-194 (2006).
9. Hagberg, H., Gressens, P. & Mallard, C. Inflammation during fetal and neonatal life: implications for neurologic and neuropsychiatric disease in children and adults. *Ann Neurol* **71**, 444-457 (2012).
10. Leviton, A., Dammann, O. & Durum, S.K. The adaptive immune response in neonatal cerebral white matter damage. *Ann Neurol* **58**, 821-828 (2005).

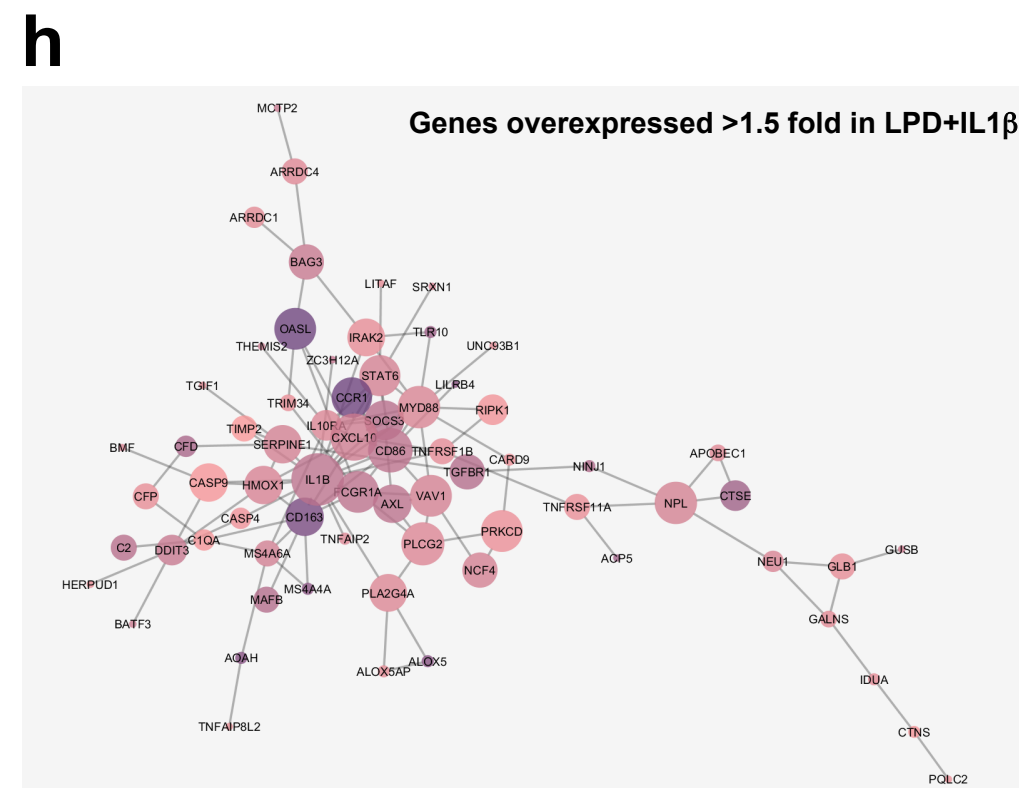
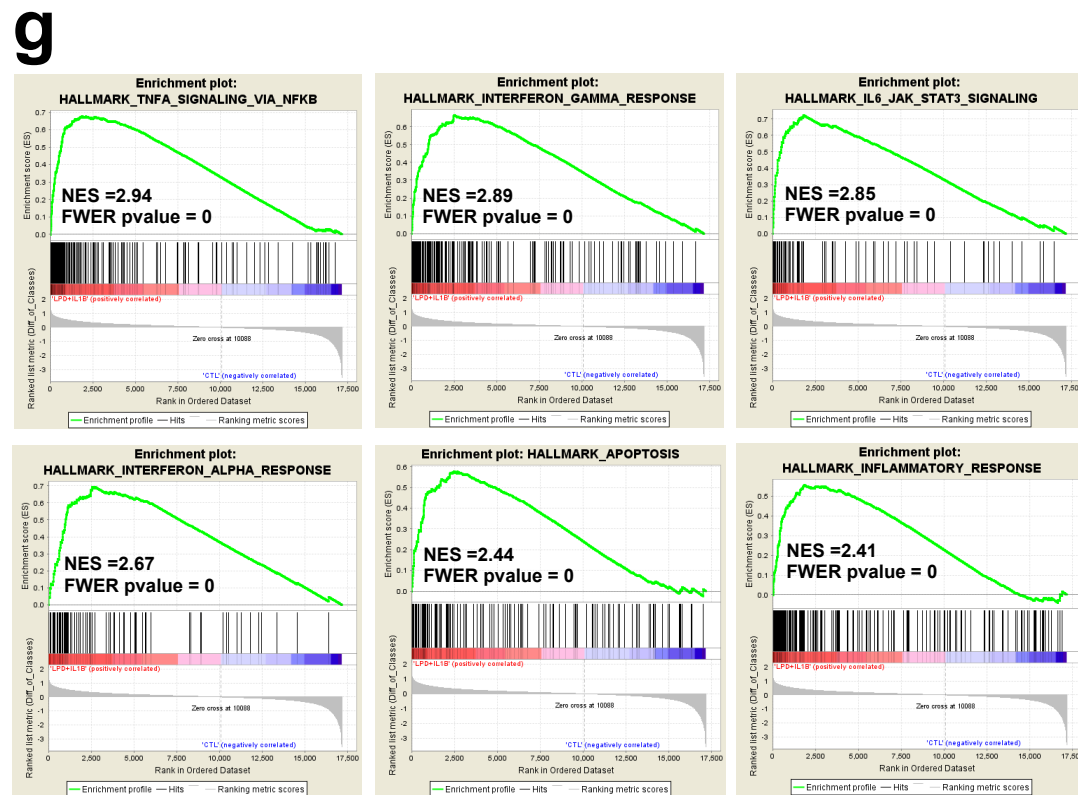
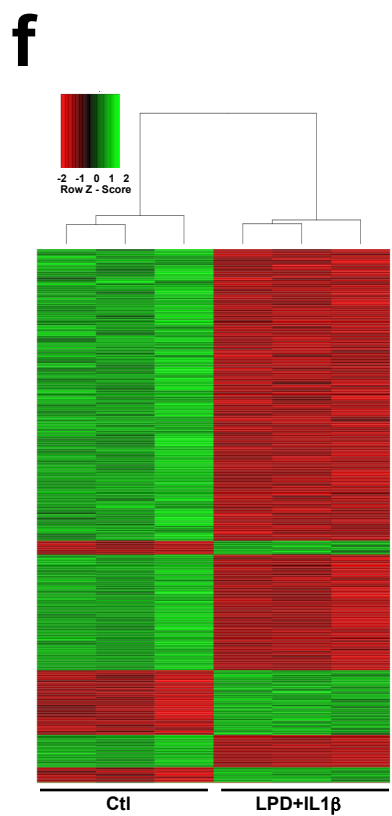
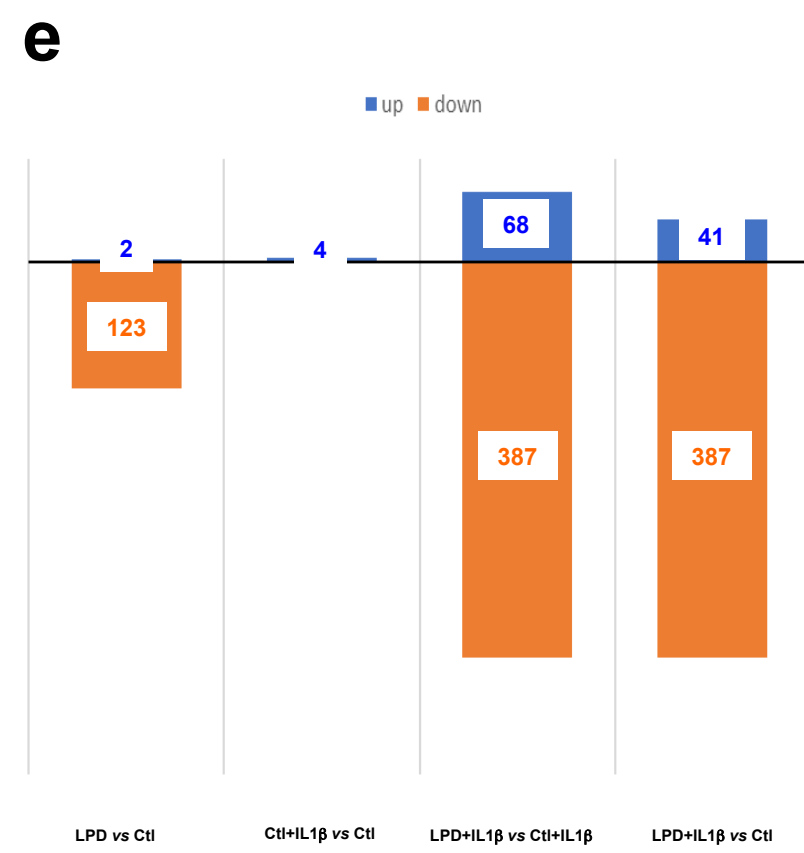
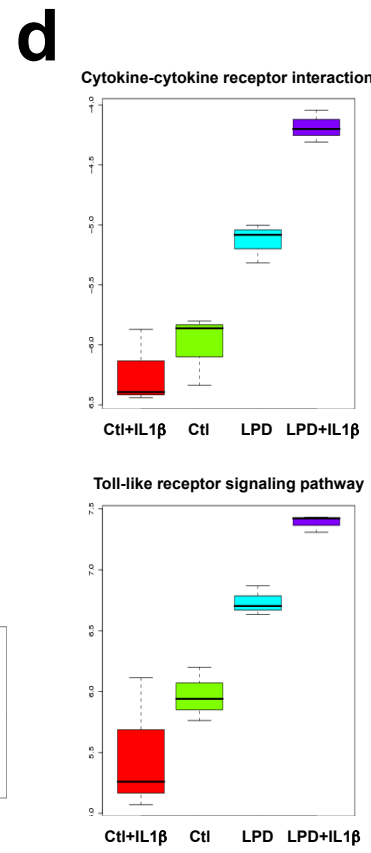
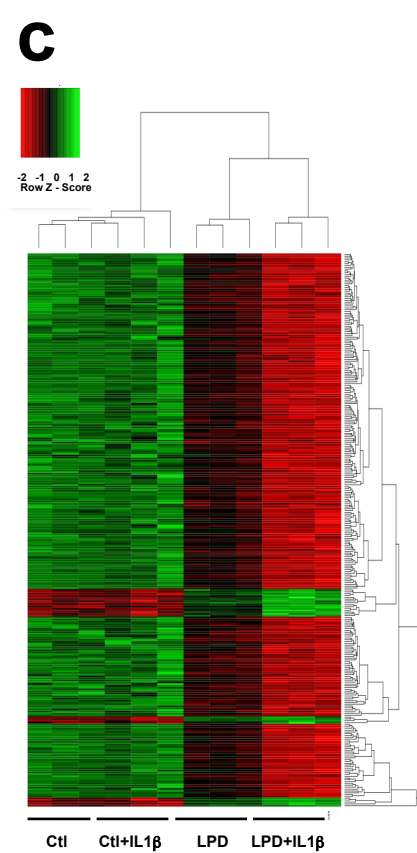
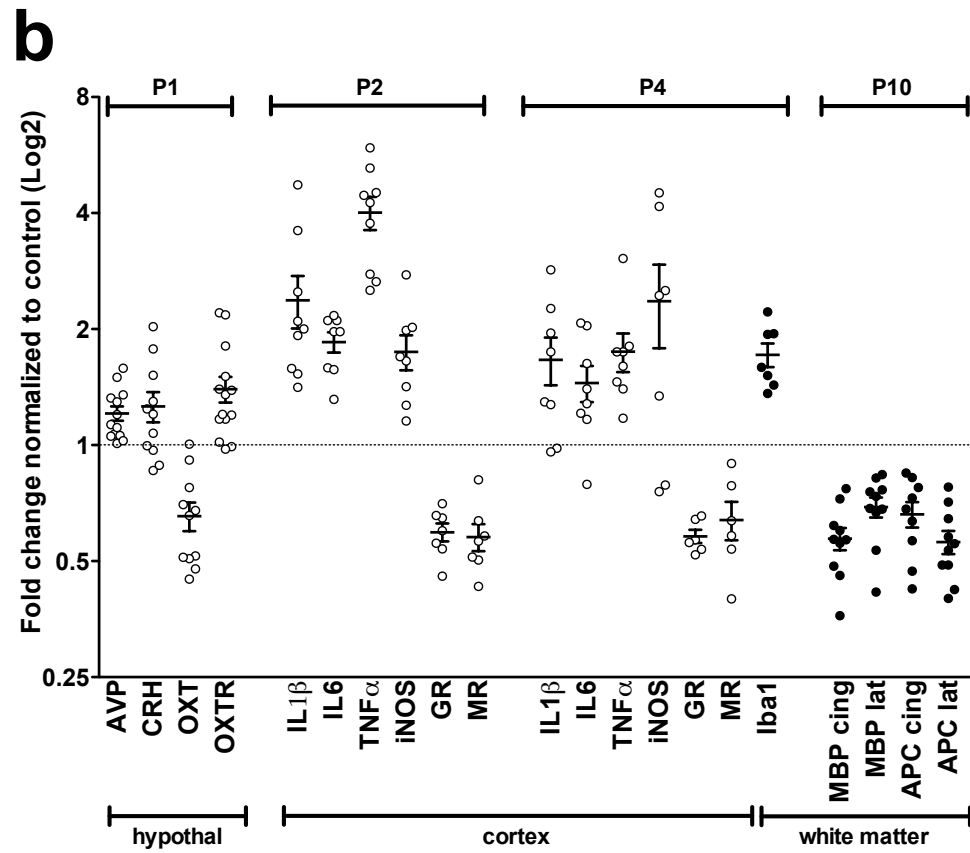
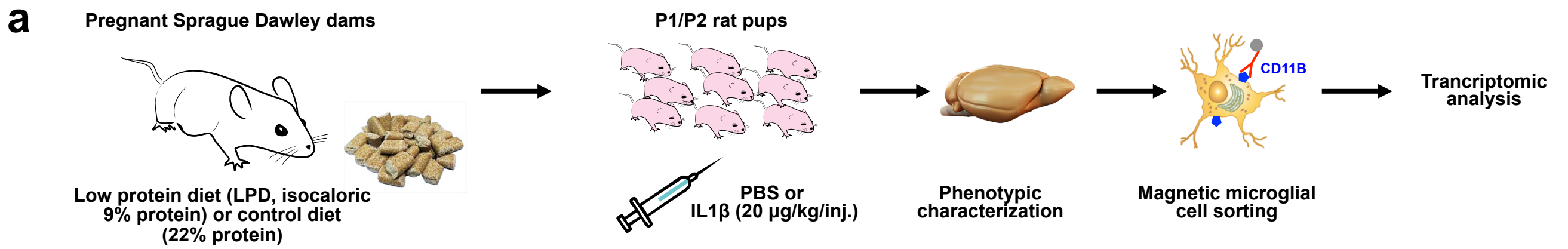
11. Rezaie, P. & Dean, A. Periventricular leukomalacia, inflammation and white matter lesions within the developing nervous system. *Neuropathology* **22**, 106-132 (2002).
12. Favrais, G., *et al.* Systemic inflammation disrupts the developmental program of white matter. *Ann Neurol* **70**, 550-565 (2011).
13. Krishnan, M.L., *et al.* Integrative genomics of microglia implicates DLG4 (PSD95) in the white matter development of preterm infants. *Nat Commun* **8**, 428 (2017).
14. Rideau Batista Novais, A., *et al.* Transcriptomic regulations in oligodendroglial and microglial cells related to brain damage following fetal growth restriction. *Glia* **64**, 2306-2320 (2016).
15. Lee, P.R., Brady, D.L., Shapiro, R.A., Dorsa, D.M. & Koenig, J.I. Prenatal stress generates deficits in rat social behavior: Reversal by oxytocin. *Brain Res* **1156**, 152-167 (2007).
16. Feldman, R. Sensitive periods in human social development: New insights from research on oxytocin, synchrony, and high-risk parenting. *Dev Psychopathol* **27**, 369-395 (2015).
17. Moisiadis, V.G. & Matthews, S.G. Glucocorticoids and fetal programming part 2: Mechanisms. *Nat Rev Endocrinol* **10**, 403-411 (2014).
18. Alkozei, A., McMahon, E. & Lahav, A. Stress levels and depressive symptoms in NICU mothers in the early postpartum period. *J Matern Fetal Neonatal Med* **27**, 1738-1743 (2014).
19. Tyzio, R., *et al.* Oxytocin-mediated GABA inhibition during delivery attenuates autism pathogenesis in rodent offspring. *Science* **343**, 675-679 (2014).
20. Romano, A., Tempesta, B., Micioni Di Bonaventura, M.V. & Gaetani, S. From Autism to Eating Disorders and More: The Role of Oxytocin in Neuropsychiatric Disorders. *Front Neurosci* **9**, 497 (2015).
21. Karelina, K., *et al.* Oxytocin mediates social neuroprotection after cerebral ischemia. *Stroke* **42**, 3606-3611 (2011).

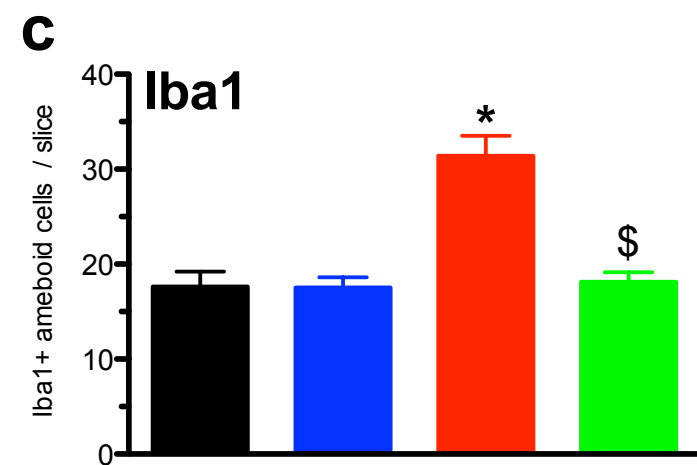
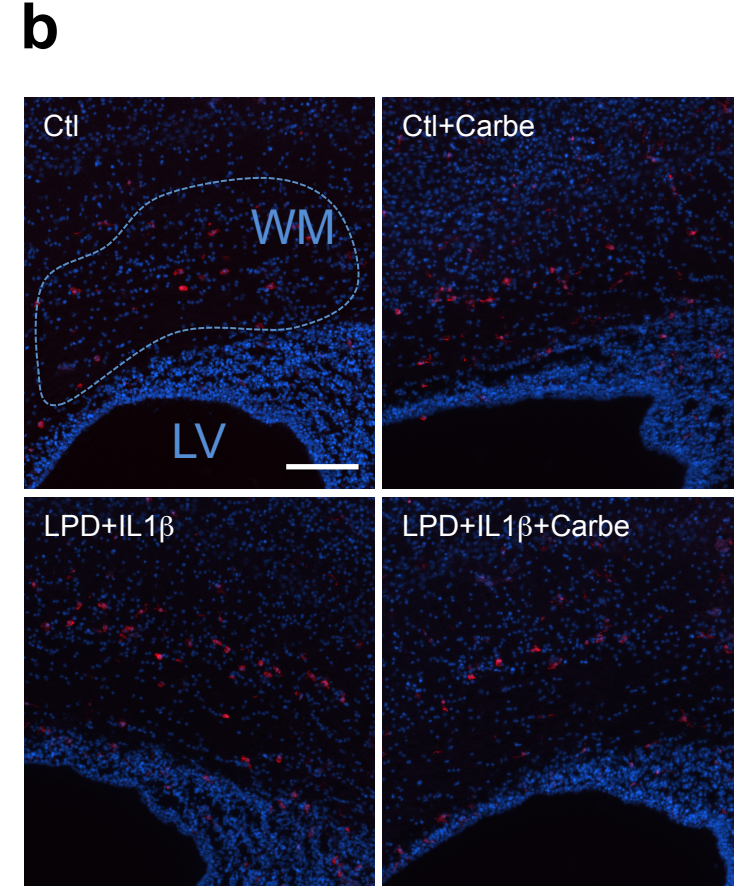
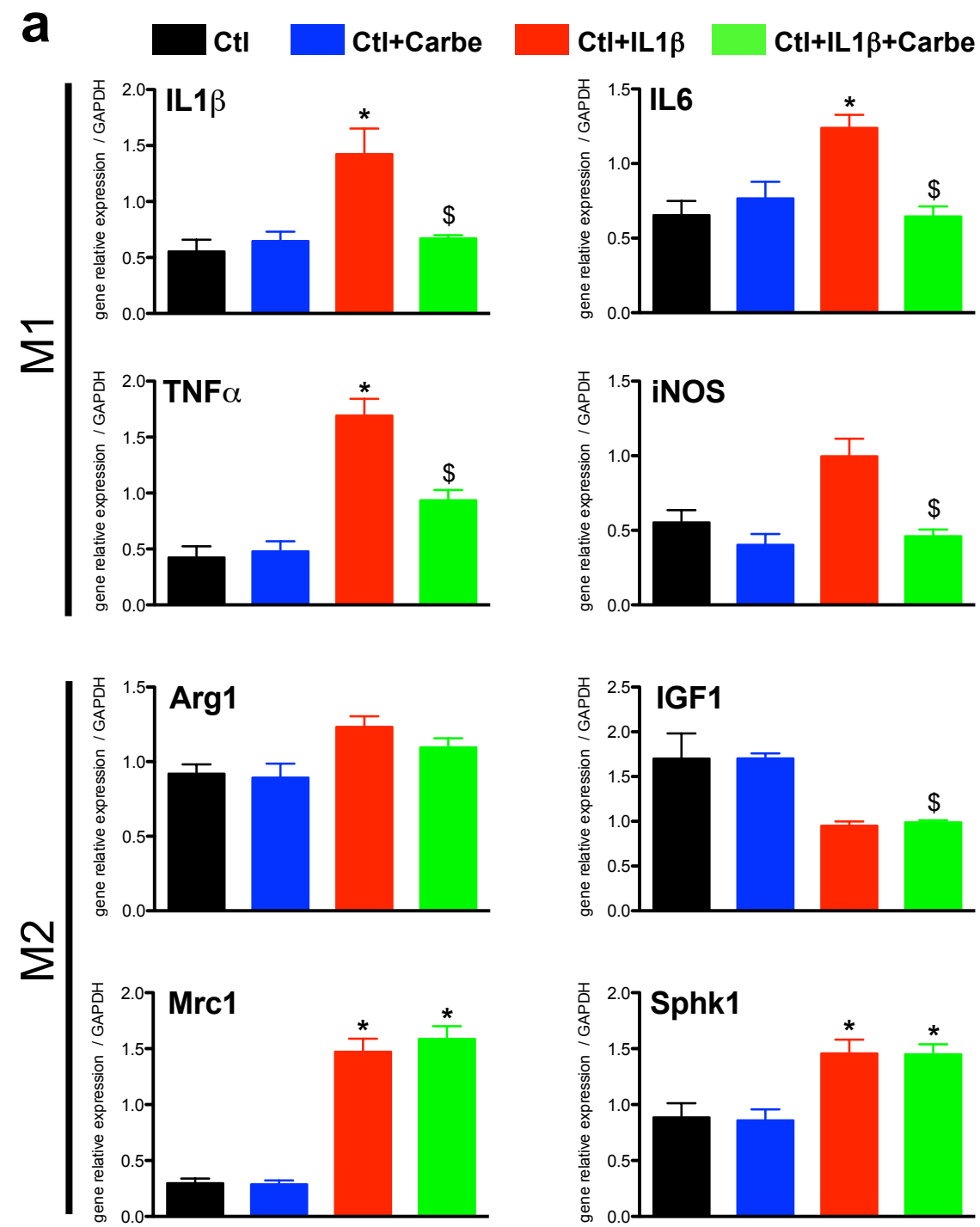
22. Yuan, L., *et al.* Oxytocin inhibits lipopolysaccharide-induced inflammation in microglial cells and attenuates microglial activation in lipopolysaccharide-treated mice. *J Neuroinflammation* **13**, 77 (2016).
23. Li, T., Wang, P., Wang, S.C. & Wang, Y.F. Approaches Mediating Oxytocin Regulation of the Immune System. *Front Immunol* **7**, 693 (2016).
24. Leviton, A., *et al.* Two-hit model of brain damage in the very preterm newborn: small for gestational age and postnatal systemic inflammation. *Pediatr Res* **73**, 362-370 (2013).
25. Subramanian, A., *et al.* Gene set enrichment analysis: a knowledge-based approach for interpreting genome-wide expression profiles. *Proc Natl Acad Sci U S A* **102**, 15545-15550 (2005).
26. Dvorska, I., *et al.* On the blood-brain barrier to peptides: effects of immobilization stress on regional blood supply and accumulation of labelled peptides in the rat brain. *Endocr Regul* **26**, 77-82 (1992).
27. Hartig, E.I., Zhu, S., King, B.L. & Coffman, J.A. Cortisol-treated zebrafish embryos develop into pro-inflammatory adults with aberrant immune gene regulation. *Biol Open* **5**, 1134-1141 (2016).
28. Peri, F. & Nusslein-Volhard, C. Live imaging of neuronal degradation by microglia reveals a role for v0-ATPase a1 in phagosomal fusion in vivo. *Cell* **133**, 916-927 (2008).
29. Babin, P.J., *et al.* Both apolipoprotein E and A-I genes are present in a nonmammalian vertebrate and are highly expressed during embryonic development. *Proc Natl Acad Sci U S A* **94**, 8622-8627 (1997).
30. Marzouk, A., *et al.* Prenatal and post-natal cost of small for gestational age infants: a national study. *BMC Health Serv Res* **17**, 221 (2017).
31. Ergaz, Z., Avgil, M. & Ornoy, A. Intrauterine growth restriction-etiology and consequences: what do we know about the human situation and experimental animal models? *Reprod Toxicol* **20**, 301-322 (2005).

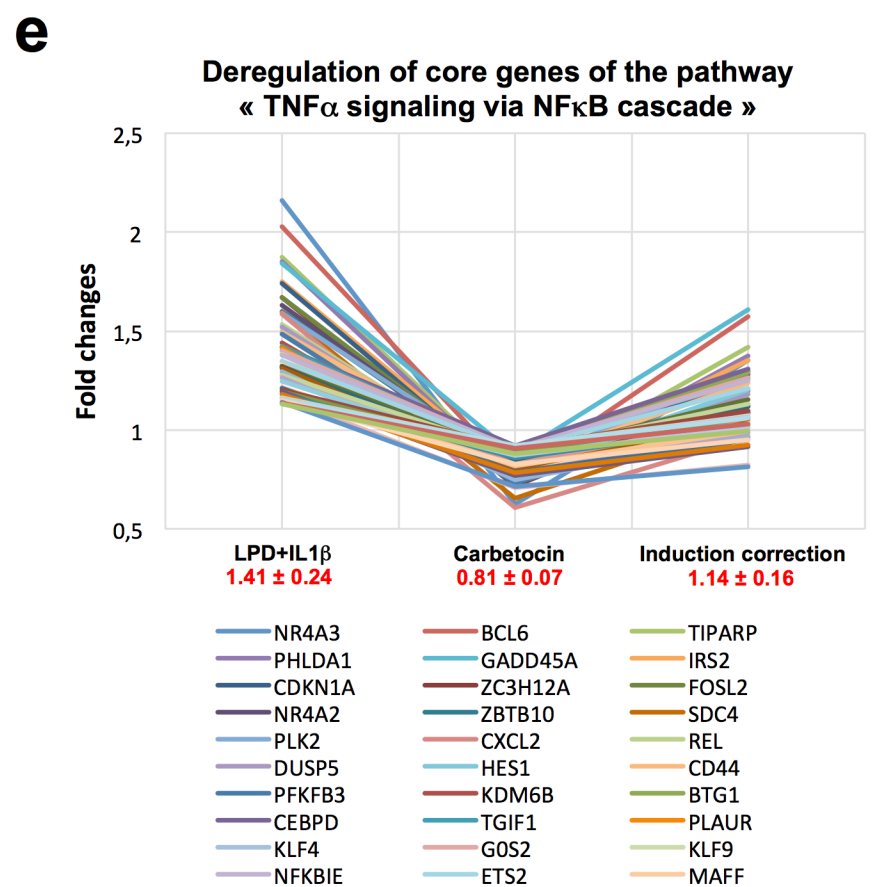
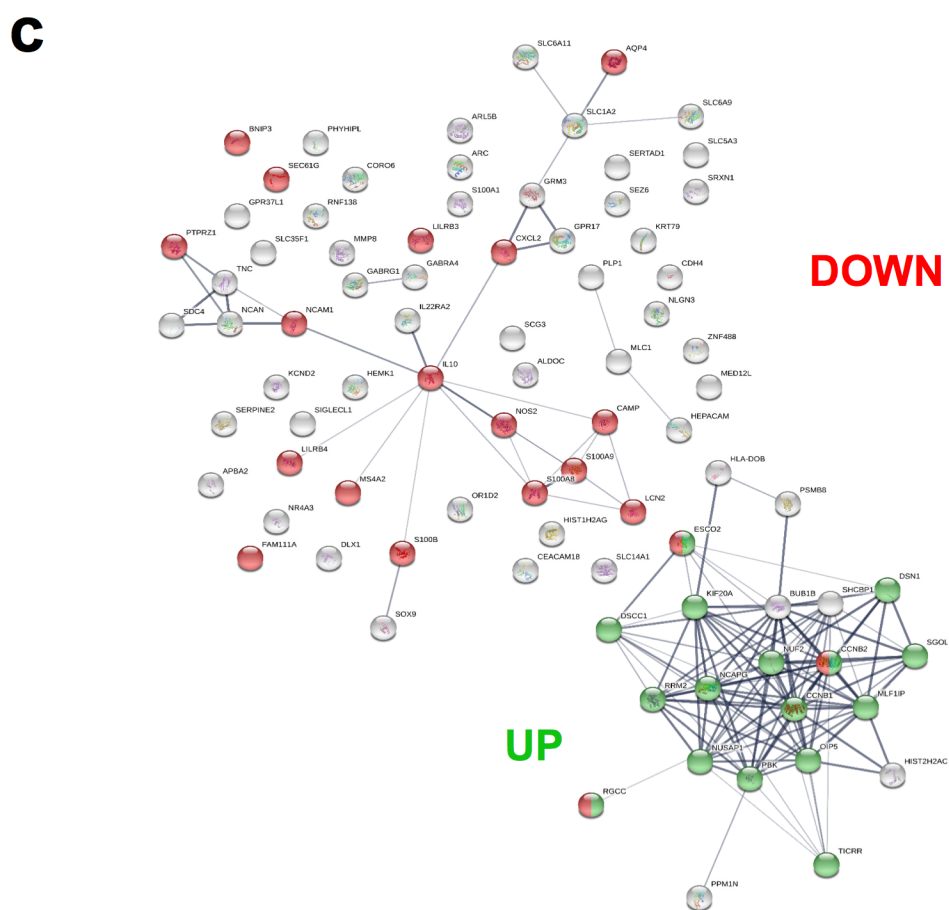
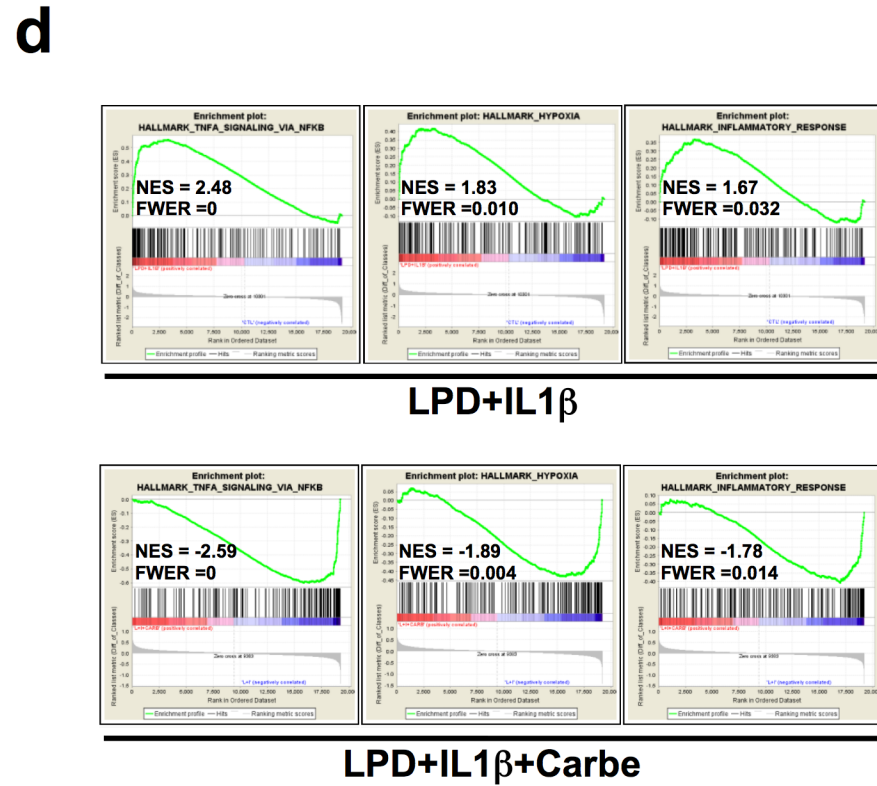
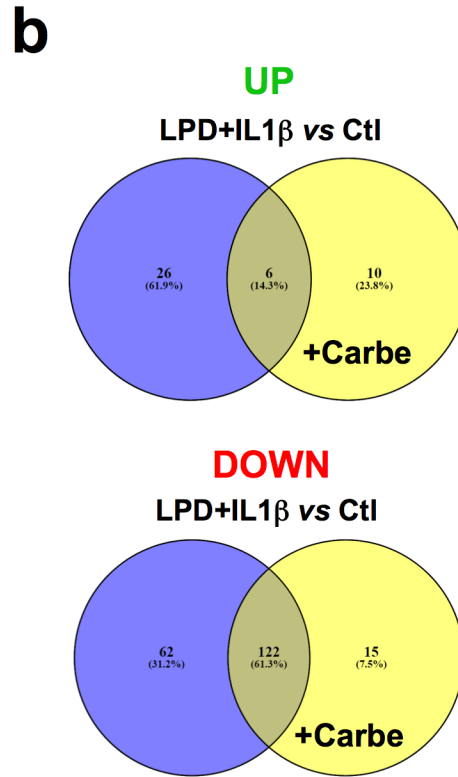
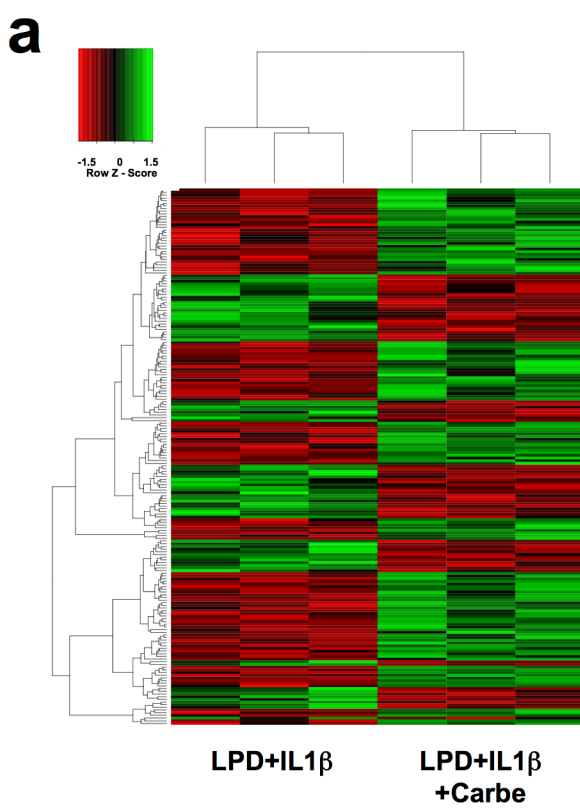
32. Miller, S.L., Huppi, P.S. & Mallard, C. The consequences of fetal growth restriction on brain structure and neurodevelopmental outcome. *J Physiol* **594**, 807-823 (2016).
33. Campbell, L.R., *et al.* Intracerebral lipopolysaccharide induces neuroinflammatory change and augmented brain injury in growth-restricted neonatal rats. *Pediatr Res* **71**, 645-652 (2012).
34. Zana-Taieb, E., *et al.* Impaired alveolarization and intra-uterine growth restriction in rats: a postnatal genome-wide analysis. *J Pathol* **235**, 420-430 (2015).
35. Boubred, F., *et al.* The magnitude of nephron number reduction mediates intrauterine growth-restriction-induced long term chronic renal disease in the rat. A comparative study in two experimental models. *J Transl Med* **14**, 331 (2016).
36. Mairesse, J., *et al.* Activation of presynaptic oxytocin receptors enhances glutamate release in the ventral hippocampus of prenatally restraint stressed rats. *Psychoneuroendocrinology* **62**, 36-46 (2015).
37. Williams, S.K. & Johns, J.M. Prenatal and gestational cocaine exposure: Effects on the oxytocin system and social behavior with implications for addiction. *Pharmacol Biochem Behav* **119**, 10-21 (2014).
38. Vanbesien-Mailliot, C.C., *et al.* Prenatal stress has pro-inflammatory consequences on the immune system in adult rats. *Psychoneuroendocrinology* **32**, 114-124 (2007).
39. Avitsur, R., Hunzeker, J. & Sheridan, J.F. Role of early stress in the individual differences in host response to viral infection. *Brain Behav Immun* **20**, 339-348 (2006).
40. Clodi, M., *et al.* Oxytocin alleviates the neuroendocrine and cytokine response to bacterial endotoxin in healthy men. *Am J Physiol Endocrinol Metab* **295**, E686-691 (2008).
41. Akman, T., *et al.* The preventive effect of oxytocin to Cisplatin-induced neurotoxicity: an experimental rat model. *Biomed Res Int* **2015**, 167235 (2015).
42. Tugtepe, H., *et al.* The protective effect of oxytocin on renal ischemia/reperfusion injury in rats. *Regul Pept* **140**, 101-108 (2007).

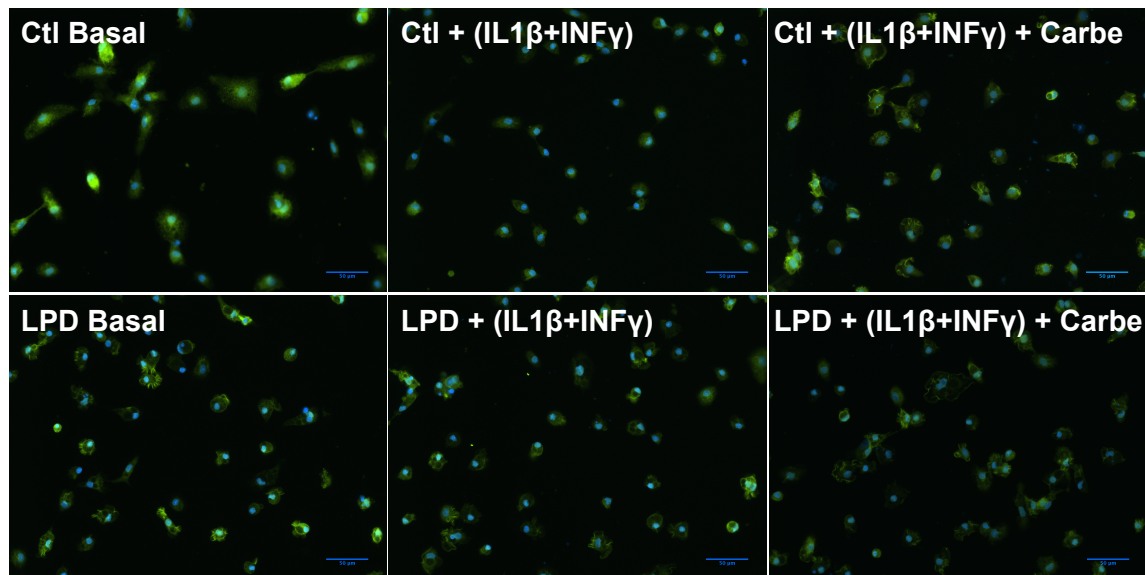
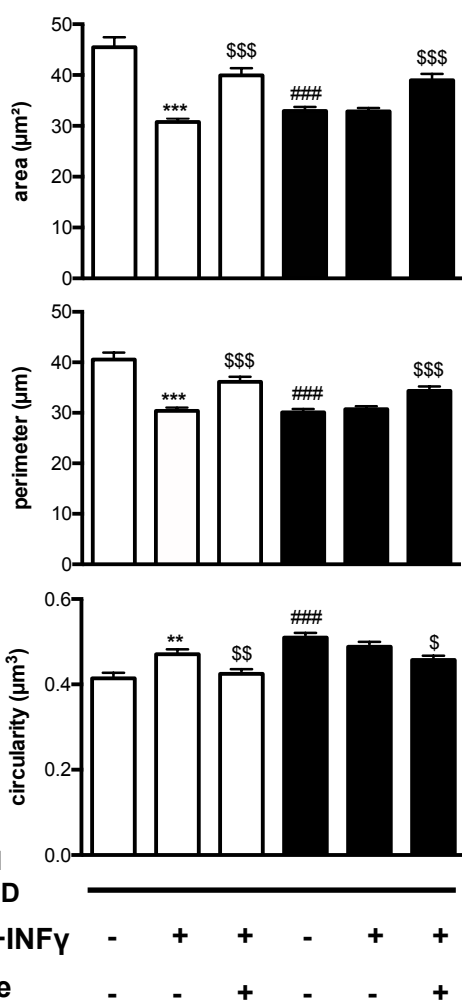
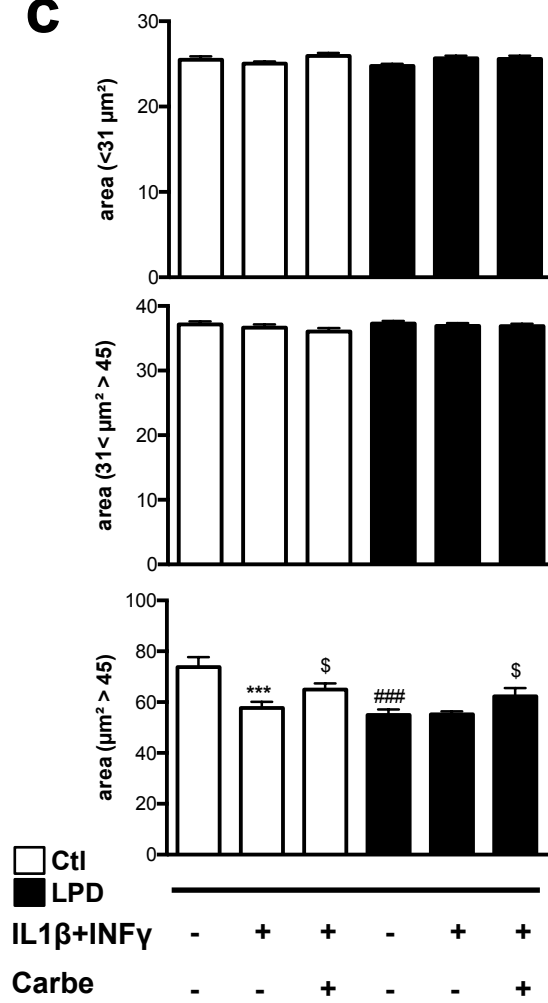
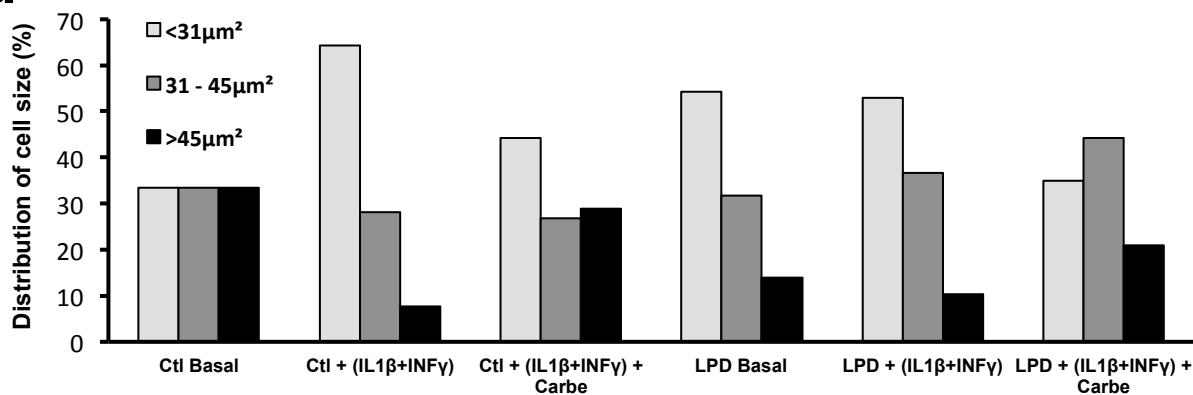
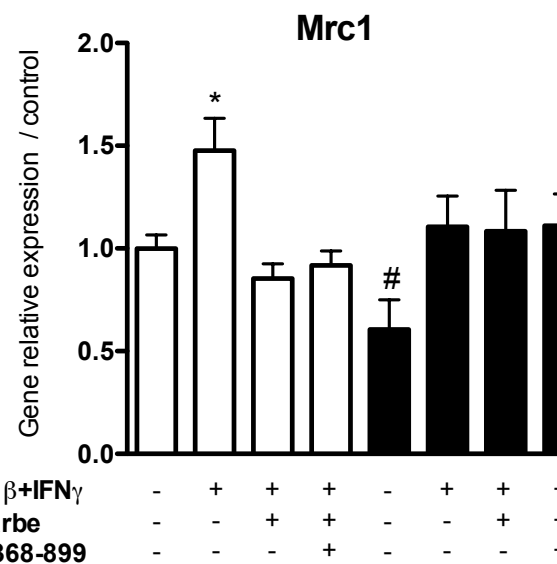
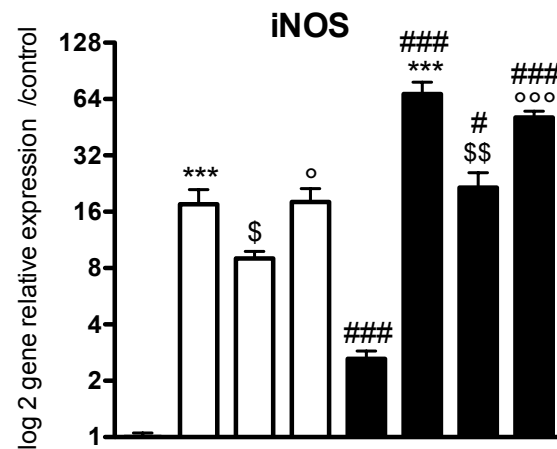
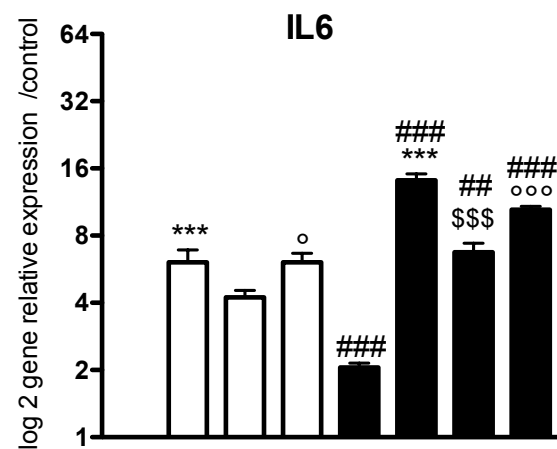
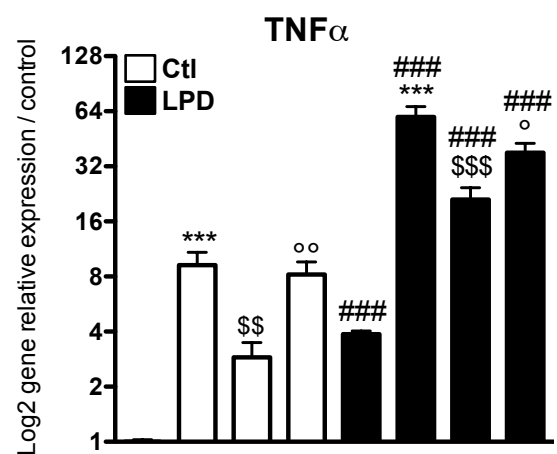
43. Szeto, A., *et al.* Oxytocin attenuates NADPH-dependent superoxide activity and IL-6 secretion in macrophages and vascular cells. *Am J Physiol Endocrinol Metab* **295**, E1495-1501 (2008).
44. Szeto, A., *et al.* Regulation of the macrophage oxytocin receptor in response to inflammation. *Am J Physiol Endocrinol Metab* **312**, E183-E189 (2017).
45. Liu, H., Leak, R.K. & Hu, X. Neurotransmitter receptors on microglia. *Stroke Vasc Neurol* **1**, 52-58 (2016).
46. Volpe, J.J. Brain injury in premature infants: a complex amalgam of destructive and developmental disturbances. *Lancet Neurol* **8**, 110-124 (2009).
47. McElrath, T.F., *et al.* Perinatal systemic inflammatory responses of growth-restricted preterm newborns. *Acta Paediatr* **102**, e439-442 (2013).
48. Dammann, O. & Leviton, A. Inflammatory brain damage in preterm newborns--dry numbers, wet lab, and causal inferences. *Early Hum Dev* **79**, 1-15 (2004).
49. Chhor, V., *et al.* Characterization of phenotype markers and neuronotoxic potential of polarised primary microglia in vitro. *Brain Behav Immun* **32**, 70-85 (2013).
50. Pierre, W.C., *et al.* Neonatal microglia: The cornerstone of brain fate. *Brain Behav Immun* **59**, 333-345 (2017).
51. Falahati, S., *et al.* Ischemia-induced neuroinflammation is associated with disrupted development of oligodendrocyte progenitors in a model of periventricular leukomalacia. *Dev Neurosci* **35**, 182-196 (2013).
52. Faustino, J.V., *et al.* Microglial cells contribute to endogenous brain defenses after acute neonatal focal stroke. *J Neurosci* **31**, 12992-13001 (2011).
53. Fernandez-Lopez, D., *et al.* Microglial Cells Prevent Hemorrhage in Neonatal Focal Arterial Stroke. *J Neurosci* **36**, 2881-2893 (2016).
54. Verney, C., *et al.* Microglial reaction in axonal crossroads is a hallmark of noncystic periventricular white matter injury in very preterm infants. *J Neuropathol Exp Neurol* **71**, 251-264 (2012).

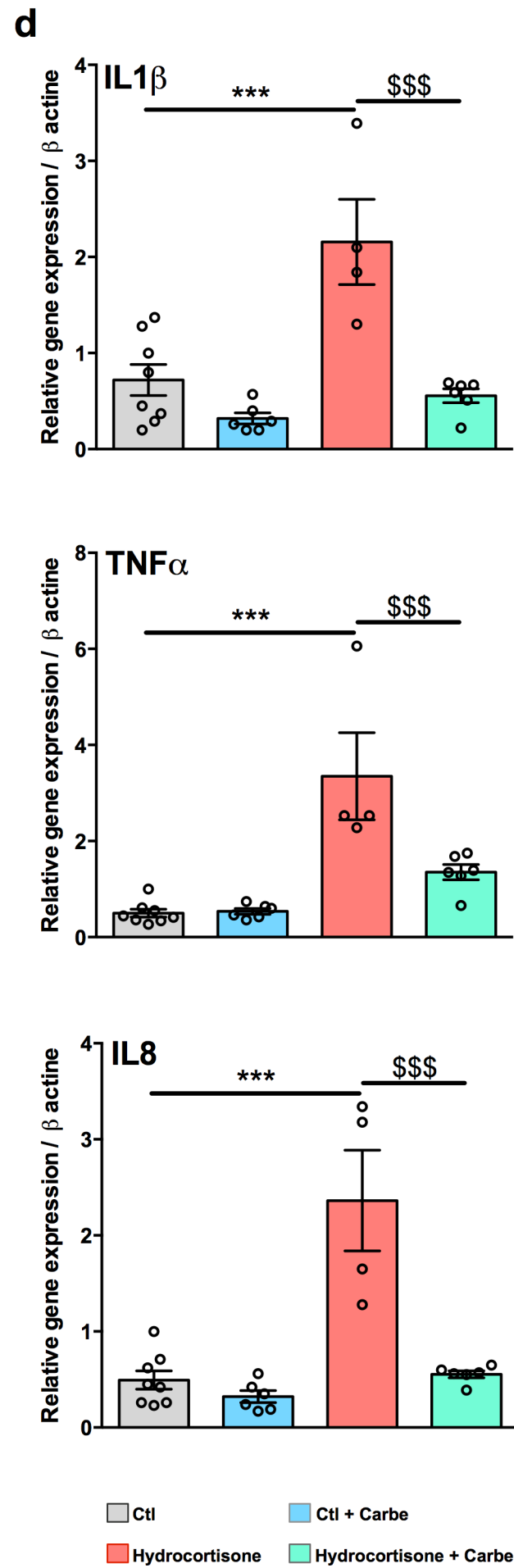
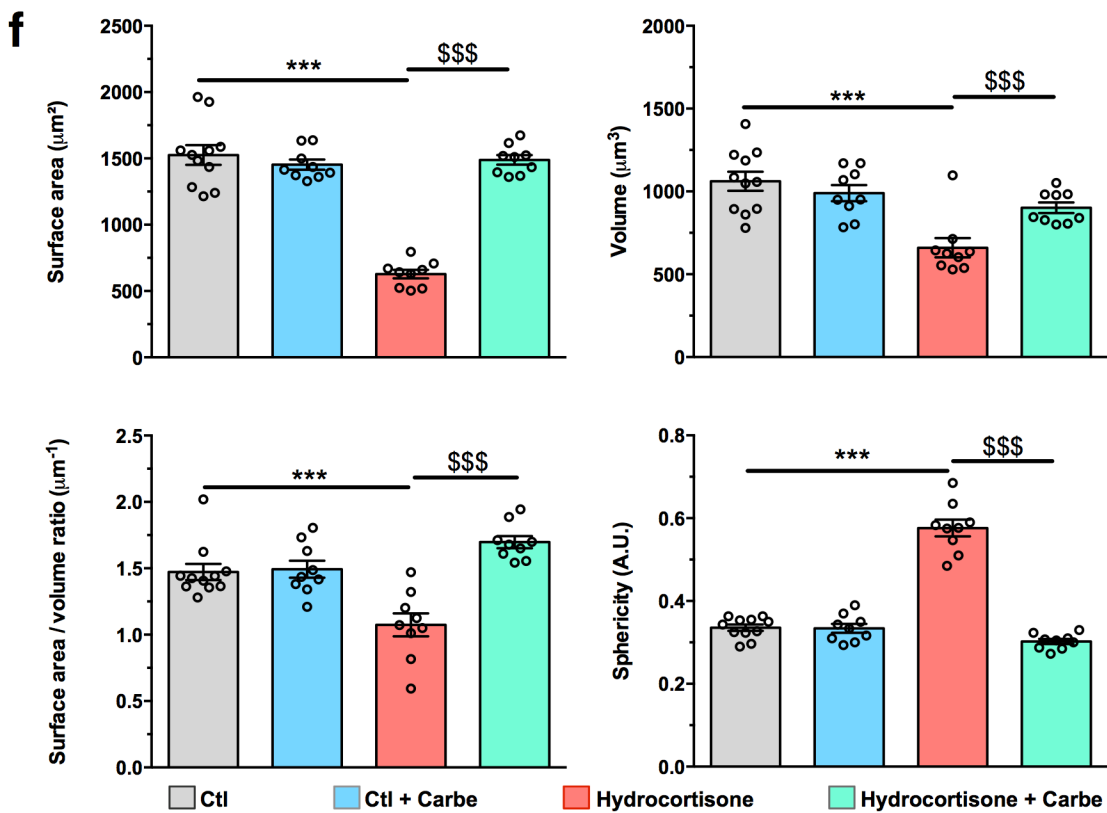
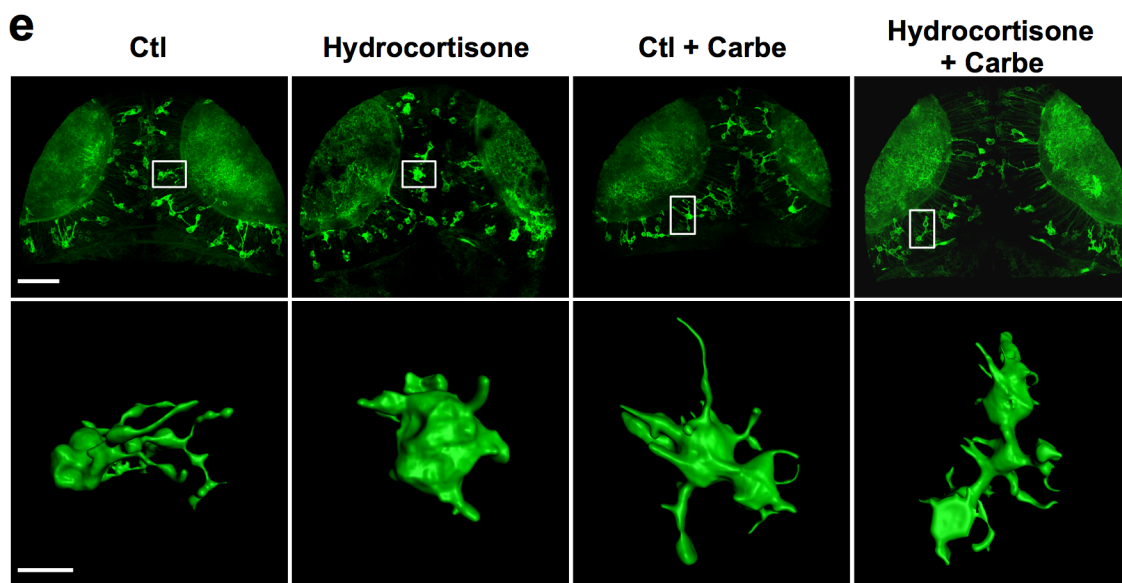
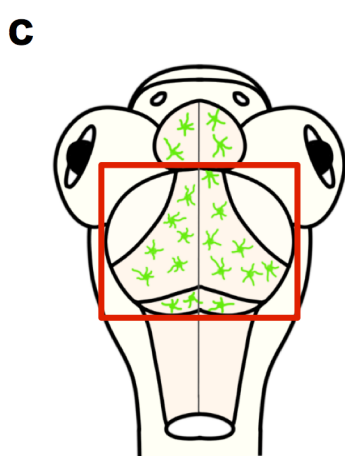
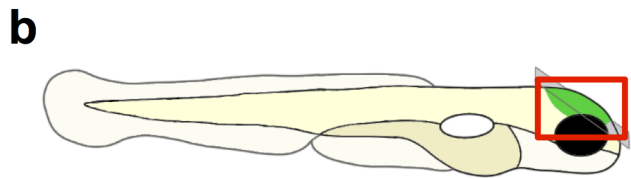
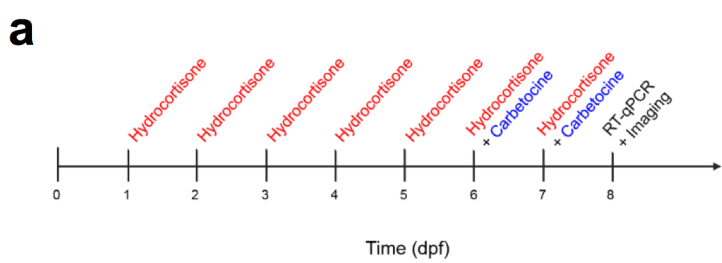
55. Hedtjarn, M., *et al.* Interleukin-18 involvement in hypoxic-ischemic brain injury. *J Neurosci* **22**, 5910-5919 (2002).
56. Burguillos, M.A., *et al.* Microglia-Secreted Galectin-3 Acts as a Toll-like Receptor 4 Ligand and Contributes to Microglial Activation. *Cell Rep* (2015).
57. Demene, C., *et al.* Functional ultrasound imaging of brain activity in human newborns. *Sci Transl Med* **9**(2017).
58. Parikh, P. & Juul, S.E. Neuroprotective Strategies in Neonatal Brain Injury. *J Pediatr* **192**, 22-32 (2018).
59. Illa, M., *et al.* Long-term functional outcomes and correlation with regional brain connectivity by MRI diffusion tractography metrics in a near-term rabbit model of intrauterine growth restriction. *PLoS One* **8**, e76453 (2013).
60. Bataille, D., *et al.* Altered small-world topology of structural brain networks in infants with intrauterine growth restriction and its association with later neurodevelopmental outcome. *Neuroimage* **60**, 1352-1366 (2012).
61. Groh, J. & Martini, R. Neuroinflammation as modifier of genetically caused neurological disorders of the central nervous system: Understanding pathogenesis and chances for treatment. *Glia* **65**, 1407-1422 (2017).
62. Salter, M.W. & Stevens, B. Microglia emerge as central players in brain disease. *Nat Med* **23**, 1018-1027 (2017).
63. Flinkkila, E., Keski-Rahkonen, A., Marttunen, M. & Raevuori, A. Prenatal Inflammation, Infections and Mental Disorders. *Psychopathology* **49**, 317-333 (2016).
64. Meziane, H., *et al.* An Early Postnatal Oxytocin Treatment Prevents Social and Learning Deficits in Adult Mice Deficient for Magel2, a Gene Involved in Prader-Willi Syndrome and Autism. *Biol Psychiatry* **78**, 85-94 (2015).
65. Penagarikano, O., *et al.* Exogenous and evoked oxytocin restores social behavior in the Cntnap2 mouse model of autism. *Sci Transl Med* **7**, 271ra278 (2015).

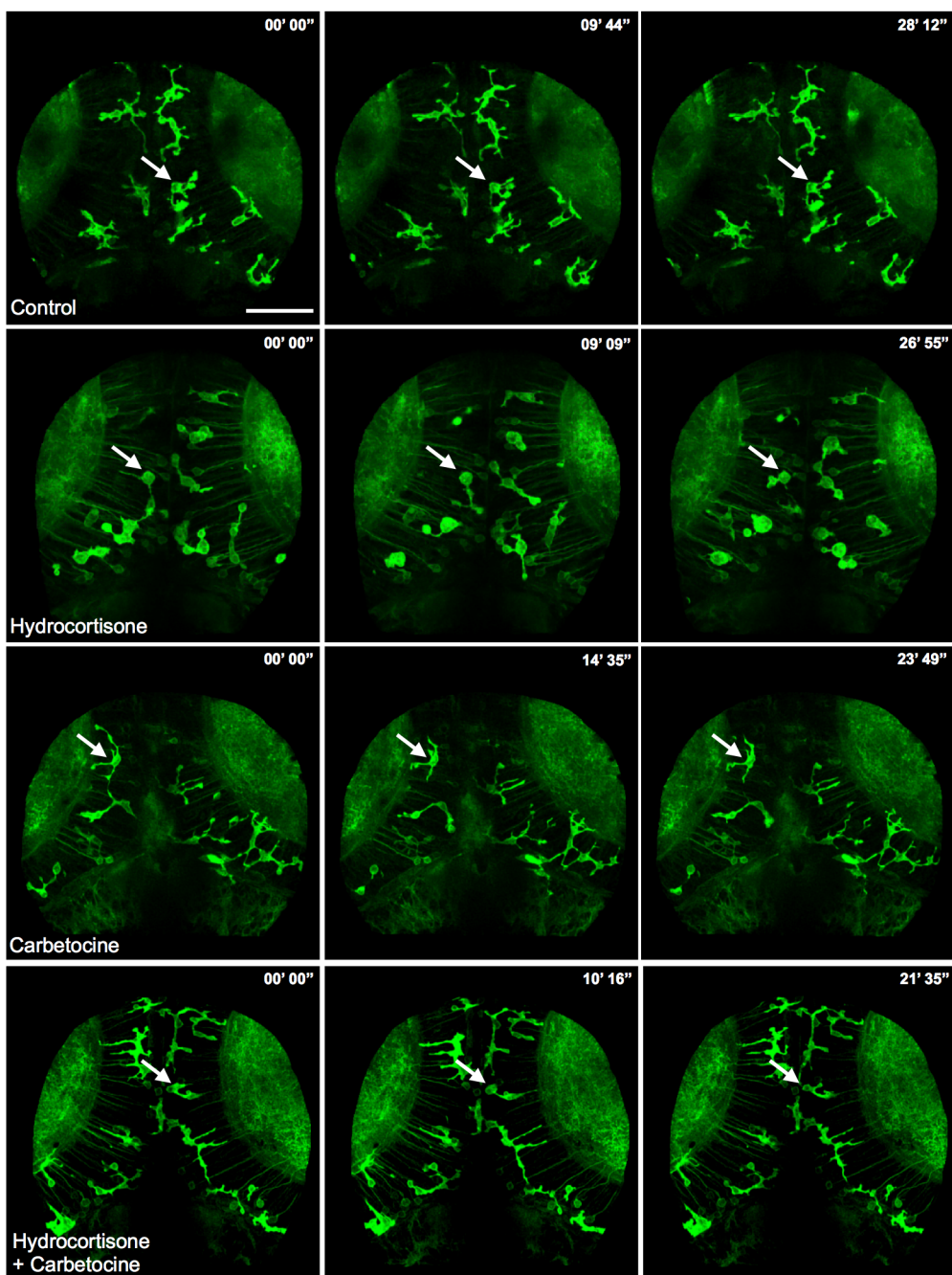
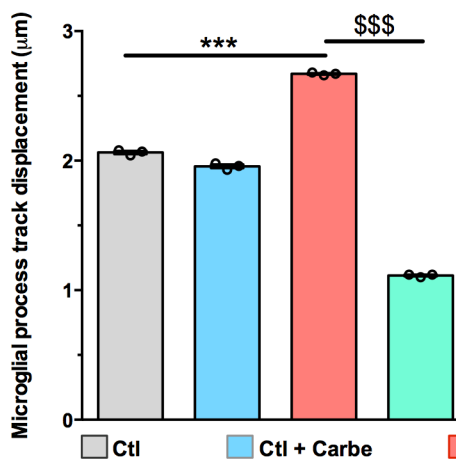
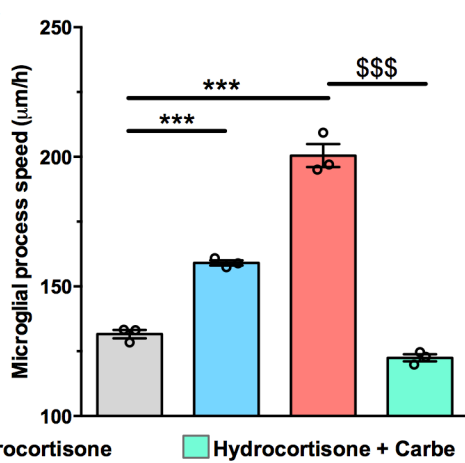


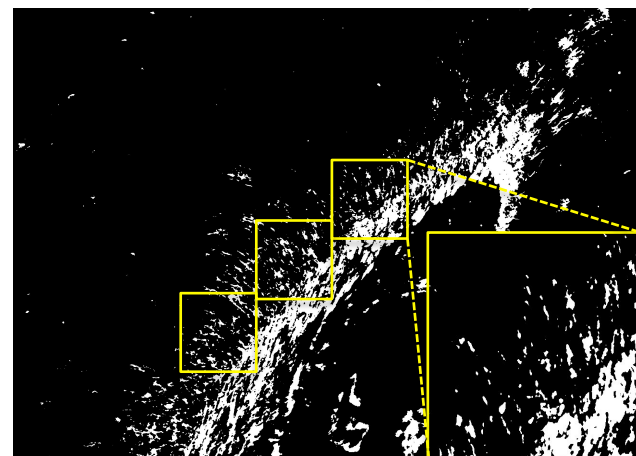
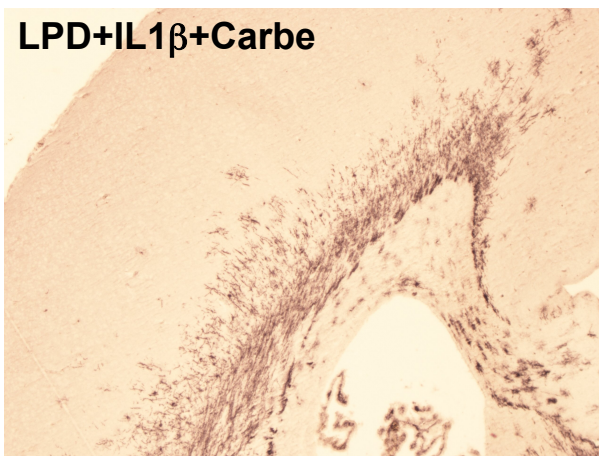
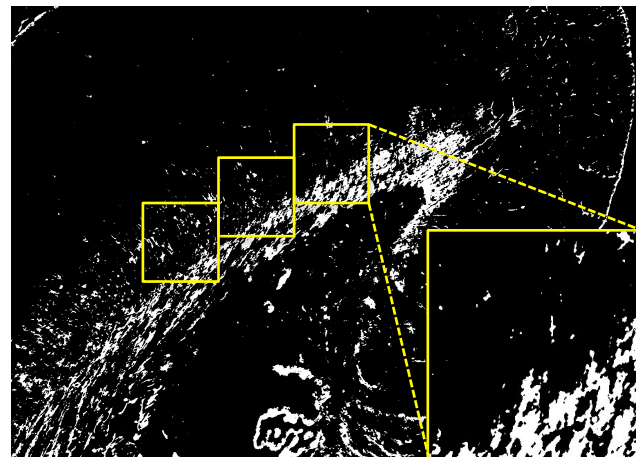
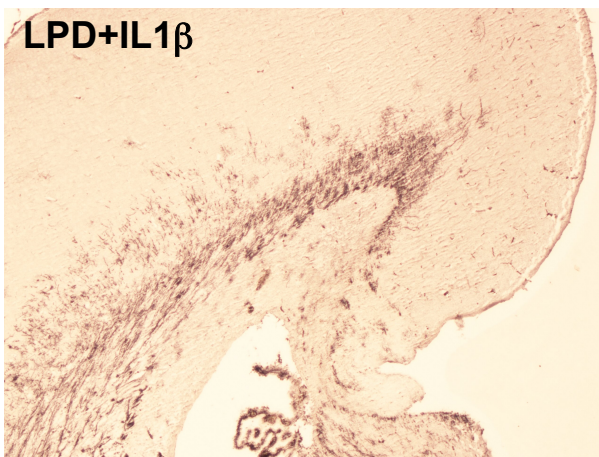
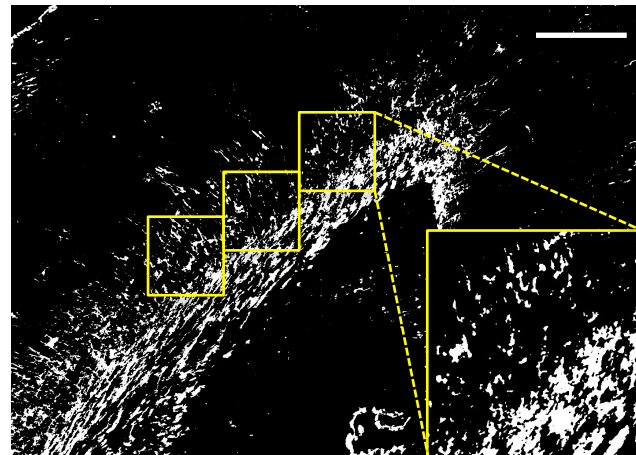
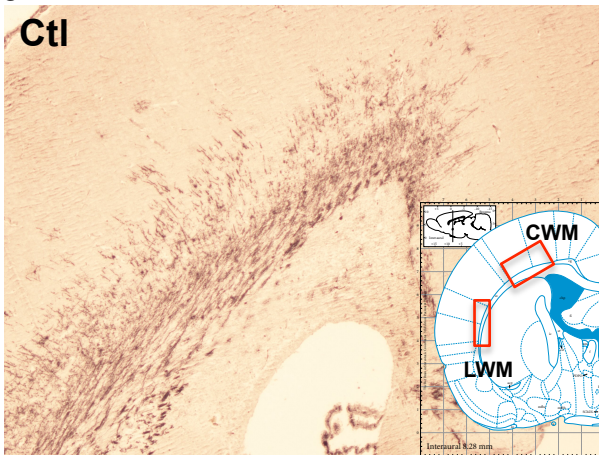
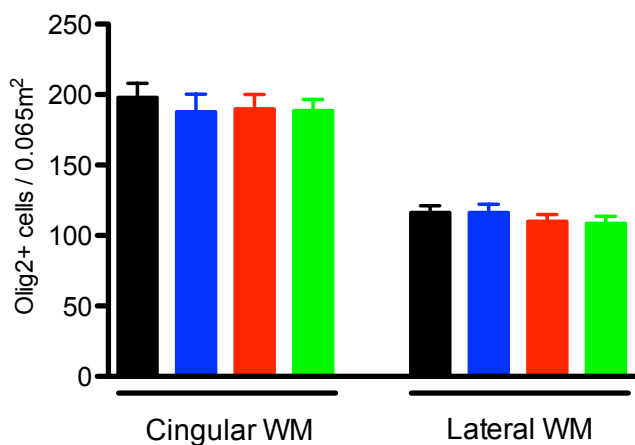
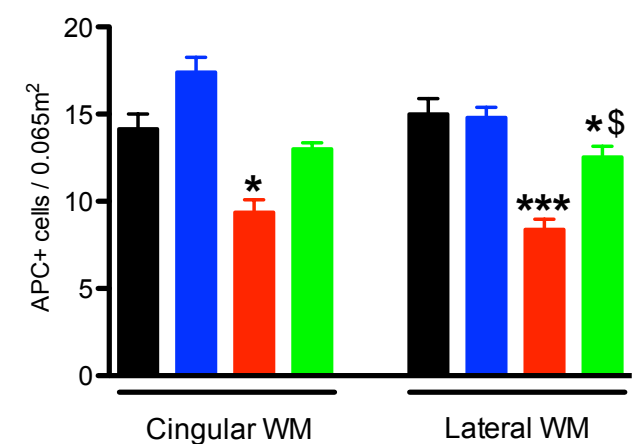
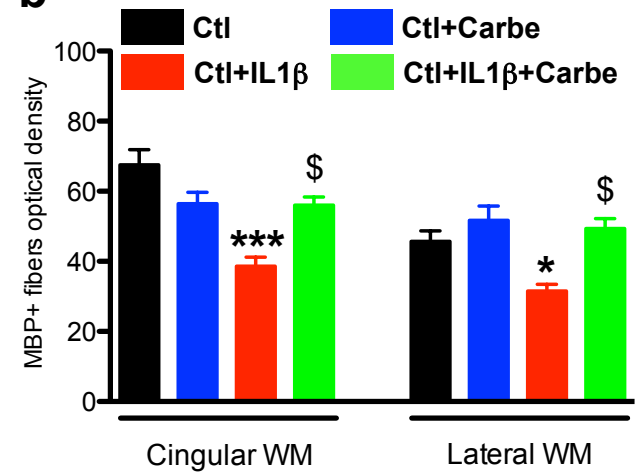


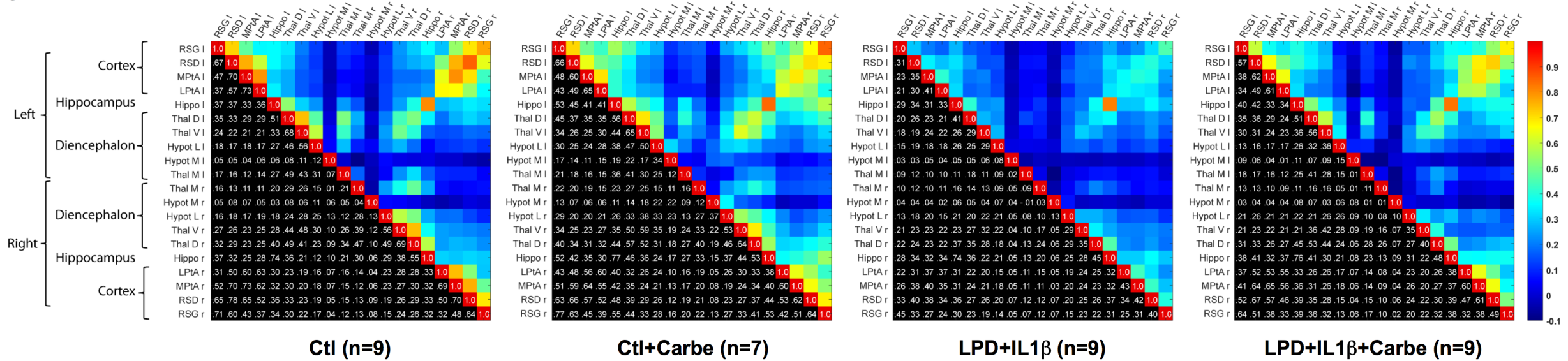
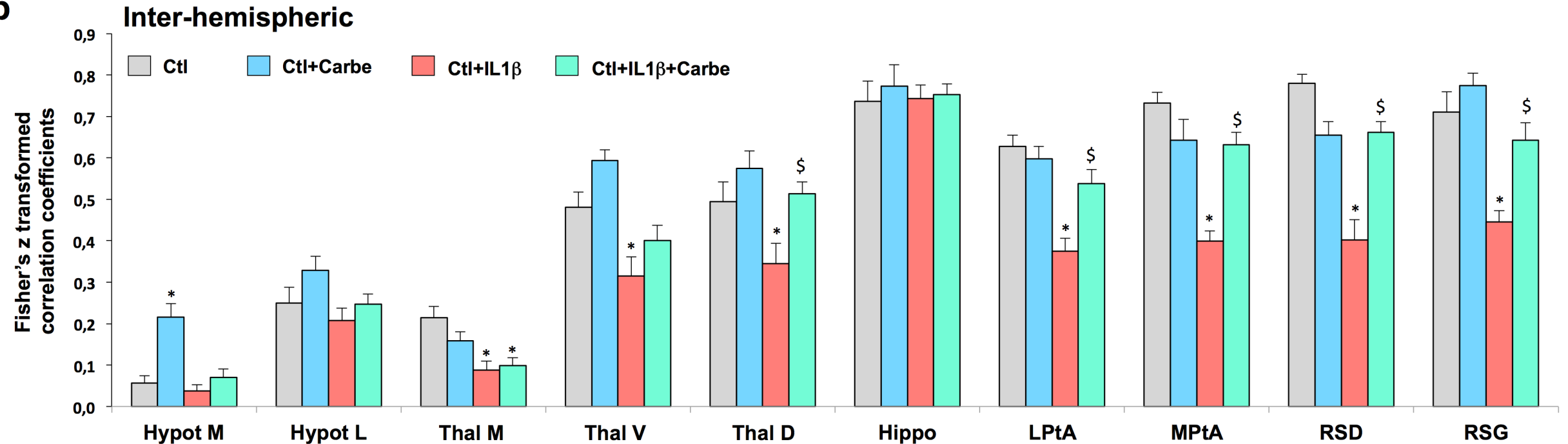
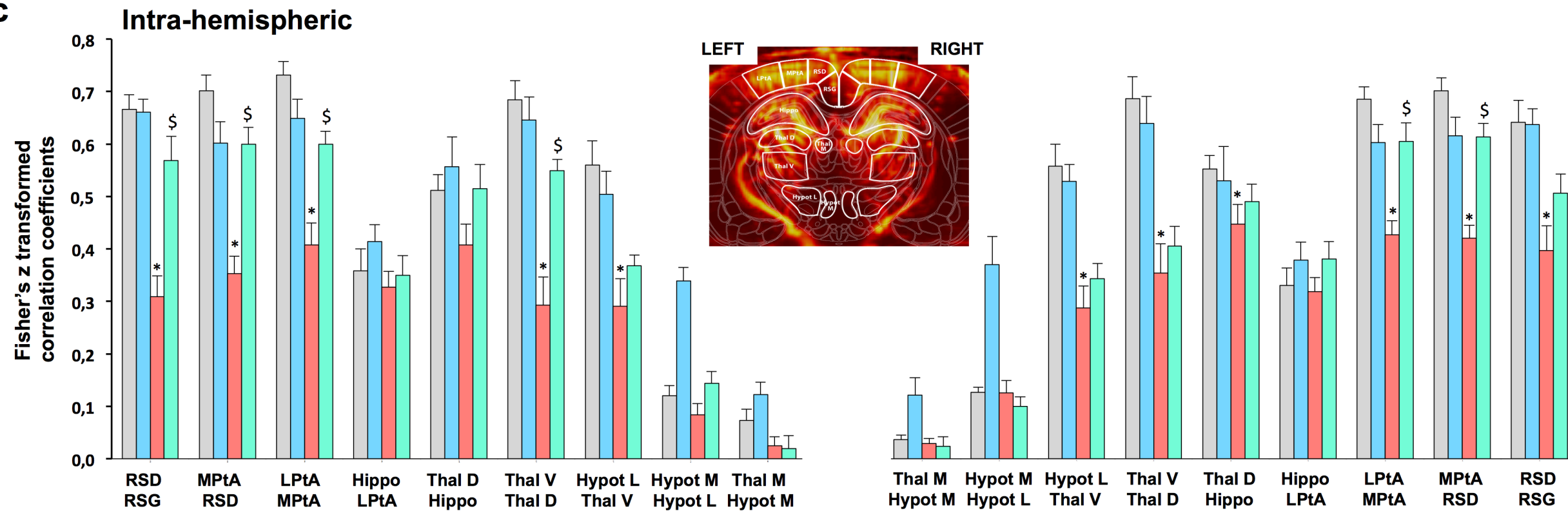


**a****b****c****d****e**

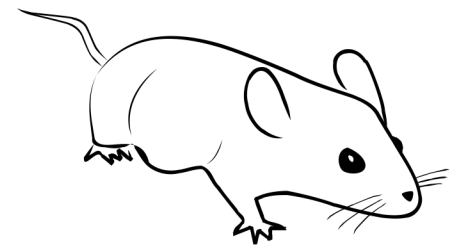


**a****b****c**

**a****b**

**a****b****c**

# Sprague-Dawley pregnant dams



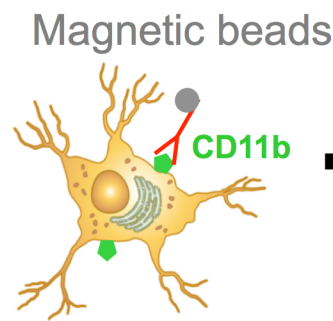
Gestation

Birth

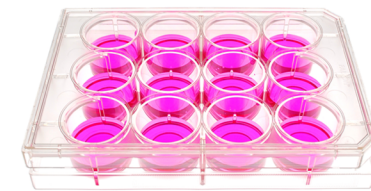
**Low protein diet (LPD)**  
(isocaloric 9% protein)  
VS  
**control diet (22% protein)**

P1 P2

Magnetic cell  
sorting of  
CD11b<sup>+</sup>  
microglia



Culture of sorted  
microglial cells



**Pro-inflammatory challenge**  
IL1 $\beta$  (50ng/ml) + INF $\gamma$  (20ng/ml)  
+/-  
Carbetocin (Oxytocin R agonist)  
L-368,899 (Oxytocin R antagonist)

*RT-qPCR,*  
*cell*  
*morphology*

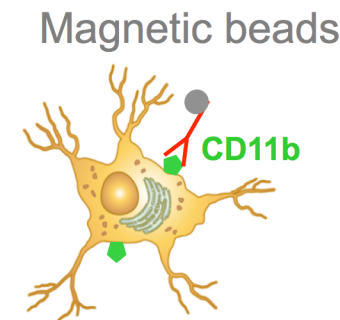
*In vitro*  
studies

P1 P2 P4

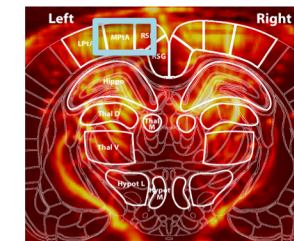
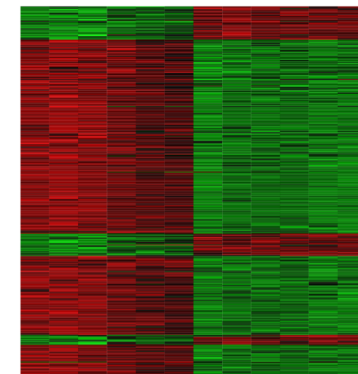
↑ ↑ ↑ ↑  
**PBS or IL1 $\beta$**   
(20 $\mu$ g/kg/12h ip)  
and/or

**Carbetocin**  
(1mg/kg/12h ip)  
↓ ↓ ↓ ↓

Magnetic cell  
sorting of  
CD11b<sup>+</sup>  
microglia



**Transcriptomic analysis**  
Microarray (Affimatrix),  
*RT-qPCR*



P1 P2 P4

↑  
**Inflammation**

P10 P21

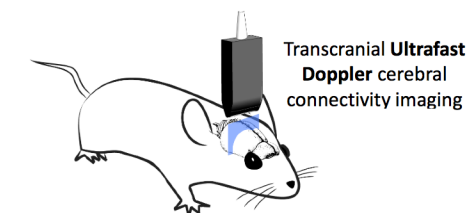
↑  
**Myelination**

P26-28

↑  
**Intrinsic Brain  
Connectivity (fUS)**

↑  
**Behavioral testing**

2 months



Transcranial Ultrafast  
Doppler cerebral  
connectivity imaging

*In vivo*  
studies

